# THE LEAKY OSCILLATOR: FORCED AND COUPLED NETWORK GAMMA

JONATHAN CANNON AND NANCY KOPELL

## 1. Introduction

[[[

TO DO LIST:

- Discuss and crop paper
- Organize appendices
- Write computational justification of timescale separation (and maybe delta)
- Caption and reference Figure 3

]]]

[[[CITE BRUMBERG2007, ERMENTROUT2001]]]

Though gamma rhythms have been studied and modeled more extensively than any other brain rhythm, the interactions of gamma-rhythmic neural circuits have received less attention. In response to widely observed synchronization between spatially separate regions of cortex and hippocampus, there has been much speculation about the entrainment of gamma-rhythmic circuits by other gamma rhythms [9][[[REFS]]], though only a few authors have treated this process within a theoretical framework [19][1] [[[MORE REFS]]]. The same observations of inter-areal synchronization have given rise to the Communication-Through-Coherence (CTC) hypothesis, stating that communication between gamma-rhythmic circuits can be modulated by their relative phase alignment, with maximally effective communication when the sender's spikes arrive at the gamma phase corresponding to minimal inhibition on the receiving population [[[FRIES AND STUFF]]]. However, the question of how such communication-facilitating coherence between populations is established and maintained remains largely unexplored. To the best of our knowledge there has been no attempt to investigate gamma entrainment and CTC within the same theoretical framework.

Here we begin to fill that gap by analyzing the basic mechanism of gamma generation in the context of the theory of forced and coupled oscillators while paying particular attention to the implications of our results for CTC. The mechanism we treat here is common to most models of gamma rhythms: the membrane potentials of a population of cells overcome slowly-decaying inhibition, causing a volley of spikes that quickly restore a high level of inhibition. As we discuss below, this process is common to models of Interneuronal Network Gamma (ING) and Pyramidal-Interneuronal Network Gamma (PING), so we refer to it as the Network Gamma (NG) mechanism, and our simple model of it as an "NG oscillator."

As our main results, we show that the NG mechanism is ideally suited to phase lock to a source of coherent pulses such that pulses arrive when inhibition is minimal; furthermore, if two NG oscillators are mutually pulse-coupled, the NG mechanism creates "dynamically directed" CTC, positioning the faster oscillator to convey information to the slower one while ignoring feedback from it. We will emphasize the fact that other oscillators do not have the properties: a generic phase locked oscillator may receive pulses at any phase, and special structure is necessary to make an oscillator with a robust period sensitive to input coherence.

**Remark 1.0.1.** *Note that "coherent" is used in two different ways here: in "communication-through-coherence," coherence refers to a consistent phase relationship between two oscillating systems, whereas a "coherent pulse" is a pulse of current that arrives concentrated within a short time window, possibly as a result of multiple small pulses temporally coinciding. We use the term "phase alignment" rather than "coherence" to refer to the first phenomenon, and reserve the term "coherence" to refer to the second, which is more consistent with its derivation from the Latin* cohaerere*, meaning "stick together."*

The rest of the paper will proceed as follows:

- In Section 2, we present and justify our model of the NG mechanism, explaining how it corresponds to the circuits underlying the generation of gamma rhythms in the brain.
- In Section 3, we discuss the basic behavior of the model from any initial conditions, and show how the pairing of slow synaptic decay coupled with leaky excitable neuronal populations creates "spike-or-forget" behavior: initial conditions are either immediately followed by a spike or immediately "forgotten" and have no influence on the next spike time. We introduce a singular limit (in which time scales of membrane dynamics and inhibition are separated) that brings this property to the forefront.
- In Section 4, the core of our mathematical work, we examine the NG oscillator's response to short excitatory pulses in its singular limit. We prove Theorem 4.2.1 stating that the phase response curve (PRC) associated with such pulses takes a specific form associated with a spike-or-forget response. We then prove Theorem 4.2.2, placing tight bounds on the height of the PRC in terms of the height of the pulse, and show that these bounds make the NG oscillator highly sensitive to pulse coherence. By contrast, we present Theorem [[[NONAME]]] (proven in Appendix [[[NONAME]]]) placing an upper bound on the PRC for a standard phase oscillator in terms of the current carried by its input, putting a limit on the effect of pulse coherence. We discuss how the NG oscillator circumvents this limitation through its special structure.
- In Section 5, we examine the NG oscillator's response to periodic pulses. We show that the spike-or-forget response of the NG oscillator creates a characteristic phase alignment with a periodic forcing pulse; furthermore, if this pulse is coherent, the NG mechanism's selectivity for coherent pulses allows it to lock to a wider range of forcing frequencies, a behavior we call "coherence filtering."
- In Section 6, we examine the dynamics of coupled NG oscillators. We show in Theorem 6.0.1 that due to the discussed characteristics of the NG mechanism, a pair of mutually-coupled non-identical NG oscillators create phase alignment optimal for directed CTC from the faster to the slower oscillator.

- In Section 7, we discuss the persistence of the NG oscillator's phase response curve for non-singularly separated time scales. We present Theorem [[[[]]] (proven in Appendix [[[NON-AME]]]) showing that the shape of these PRCs do persist in such a way that our results hold for small but nonzero separation of time scales, and we present numerical simulations as additional support.

## 2. The NG Mechanism

Two classes of circuits are known to create gamma rhythms. The first and simplest, the Interneuronal Network Gamma (ING) circuit, consists a population of interneurons synaptically networked to inhibit itself. The second, the Pyramidal-Interneuronal Network Gamma circuit, comprises a population of excitatory pyramidal cells (E-cells) reciprocally synaptically connected with a population of inhibitory interneurons (I-cells), both of which may also synaptically target themselves. Both circuits generate rhythms by the following process:

- Inhibition on a quiescent population of cells (I-cell in ING, or E-cells in PING) decays slowly.
- Some portion of this population is driven to spike at approximately the same time due to tonic excitation.
- As a result of this volley of spikes, inhibitory synapses quickly increase towards maximal saturation, and the population returns to quiescence. (In the PING circuit, E-spikes cause inhibition by exciting I-cells and triggering I-spikes.)

We shall refer to this mechanism of rhythm generation as the NG (Network Gamma) mechanism. Here we study a simple model that generates rhythms by NG. We will not concern ourselves with the causes of gamma synchronization and desynchronization, which have been extensively studied in [21], [12], [3], [6], [14], [8], and [7]; instead, we will consider only populations that fulfill the conditions for sustained synchrony by one of the mechanisms identified by these authors.

### 2.1. The NG Model.

We will study a simple two-dimensional model that captures NG mechanism without any unnecessary detail. Due to its generality and suitability for representing the NG mechanism in its simplest form, we shall refer to this system as the "NG oscillator." We let $V$ denote the membrane potential of the population (assumed to be shared by all cells), and we let $s$ denote the saturation of the inhibitory synapses to each cell (again assumed to the the same for all cells) as a fraction in $[0, 1]$. We use a Quadratic Integrate-and-Fire (QIF) model to describe the evolution of the membrane potential, and assume exponential synaptic decay with rate constant $\tau_s$:

$$\begin{cases} \dot{V} = & \frac{1}{\tau}(V^2 + G) \\ \dot{s} = & -\frac{s}{\tau_s} \end{cases} \tag{1}$$

where

$$G = b - gs + I(t)$$

is the net flux of current; $g$ is the maximal conductance of the I-cell autapse; $\tau_s$ is the decay time constant of inhibition; $\tau$ is the I-cell membrane time constant; $b > 0$ is the baseline level of tonic excitation of the I-cell; and $I(\cdot) > 0$ is any additional synaptic current delivered to the I-cell as a function of time. We treat the synaptic current as an injected current with no reversal potential; we show in the next section that the introduction of a reversal potential would not qualitatively change our results.

When $V$ reaches $V_{spike} \in (0, \infty]$, it "spikes" and resets to $V_{reset} \in [-\infty, 0)$. At a spike, $s$ resets instantly to 1. Similar equations were used to model forced gamma rhythms in [4].

**Remark 2.1.1.** *If $V_{spike} = \infty$, a spike is a finite-time blow-up of $V$. If $V_{reset} = -\infty$, the trajectory of $V$ after a spike at time 0 is the unique trajectory obeying the ODE and approaching $-\infty$ in its limit at time 0.*

**Remark 2.1.2.** *Under some conditions, it is also possible to perform the following analysis on a system in which $s$ resets as a function $\rho(s)$ of its value at each spike. One natural choice would be*

$$\rho(s) = s + d. \tag{2}$$

*for some increment $d$. This map is used in the theta neuron with adaptation presented in [13]. It ignores the effect of synaptic saturation, which may be justified in a regime in which inhibitory synapses were not close to saturation. Another natural choice would be*

$$\rho(s) = 1 + c(s - 1) \tag{3}$$

*for some $c \in [0, 1)$. In a companion paper [[[Paper 1ac]]], we show that this resetting map $\rho$ is a natural simplification of the fast rise-time behavior of standard model synapses [[[NAME???]]]. In the remainder of the paper, our choice of resetting function is equivalent to setting $c = 0$; we make this choice for the simplest possible presentation of our main ideas.*

We use subscript to refer to the value of a variable at a certain time: e.g., $V_t$, $s_t$, $G_t$.

2.2. **The NG model rescaled.** We nondimensionalize our model by rescaling $t$ into units of $\tau$. We set $\mu := \frac{\tau}{\tau_s}$ and rewrite (1) as

$$\begin{cases} \frac{\partial}{\partial \check{t}} V = & V^2 + G \\ \frac{\partial}{\partial \check{t}} s = & -\mu s \end{cases} \tag{4}$$

where

$$G = b - gs + I(\tau \check{t}).$$

2.3. **Extension to PING.** Our model also captures the basic behavior of PING. In the PING cycle, E-cells rise above the inhibition and emit an excitatory spike volley, which quickly triggers an inhibitory spike volley. We may treat them as if every time they spike, they inhibit themselves with a short, slightly variable delay. When excitatory forcing or coupling is delivered to the E-cells, the timing of spike volleys is determined entirely by the dynamics of inhibition and E-cell membrane potential, which may be approximated by the two-dimensional model (1) using $V$ to represent the membrane potential of the E population and $s$ to represent the level of inhibition. We discuss this correspondence more fully in the companion paper [[[Paper 1ac]]], and demonstrate that if the

I-cells have sufficiently short time constants, then the dynamics of PING under excitatory E-cell forcing do not differ qualitatively from those of forced ING.

One significant difference between PING and the basic NG model arises when forcing is delivered to I-cells as well as E-cells. See Remark 7.1 [[[AND APPENDIX?]]] for discussion of the differences this may cause.

## 3. Model behavior

*Here we study the behavior of the NG model by separating the behavior on time scales $\tau$ and $\tau_s$.*

When the NG mechanism is unforced, i.e., $I(\cdot) = 0$, all initial conditions flow into a single attracting periodic orbit: from any set of initial conditions $(V_0, s_0) \in \mathbb{R} \times [0, 1]$, $s$ eventually decays below $\frac{b}{g}$ and $G$ becomes positive, at which point $V$ spikes, $(V, s)$ is reset to $(V_{reset}, 1)$, and the remainder of the trajectory follows the stable limit cycle issuing from $(V_{reset}, 1)$. See Figure 2, left, for illustration.

In the remainder of this section, we will assume $\tau \ll \tau_s$, i.e., $\mu \ll 1$. This assumption is justified by the observation that cells participating in gamma oscillations are in a state of high background conductance, and therefore have severalfold shorter membrane time constants than they do at rest [**Destexhe2003a**][**Economo2012**]. (Also, fast-spiking interneurons are characterized by short membrane time constants even in low-conductance states [**Pike2000**]). We make this assumption in order to quantitatively capture and explain two aspects of the behavior of the NG mechanism:

(1) Membranes reach their stable resting potential quickly and follow it closely as $G$ changes.

(2) When the membrane potentials are driven past threshold, a spike volley occurs shortly afterwards.

The analysis we perform based upon the assumption of small $\mu$ applies to an NG process to the extent that it exhibits these two behaviors. Later we demonstrate that a simulation with only a modest separation of the two time constants produces similar results.

**Remark 3.0.1.** *As demonstrated by Kilpatrick and Ermentrout in [15], the NG system without forcing can be solved with Bessel functions. However, the results we are interested in are closely related to the separation of timescales, so we forgo the study of this system by direct solution in favor of a more intuitive singular-perturbation-style approach.*

3.1. **The fast subsystem.** We let $\mu \to 0$ in (4) to describe the fast membrane dynamics of the ING oscillator:

$$\begin{cases} \frac{\partial V}{\partial t} = & V^2 + G \\ \frac{\partial s}{\partial t} = & -\mu s \approx 0 \end{cases} \tag{5}$$

In this "fast subsystem," $s$ is constant, so if no input arrives, $G$ is also constant. If $G < 0$, the ODE for $V$ has two fixed points that can be expressed as functions of $G$:

$$V^{\pm}(G) = \pm\sqrt{-G} \tag{6}$$

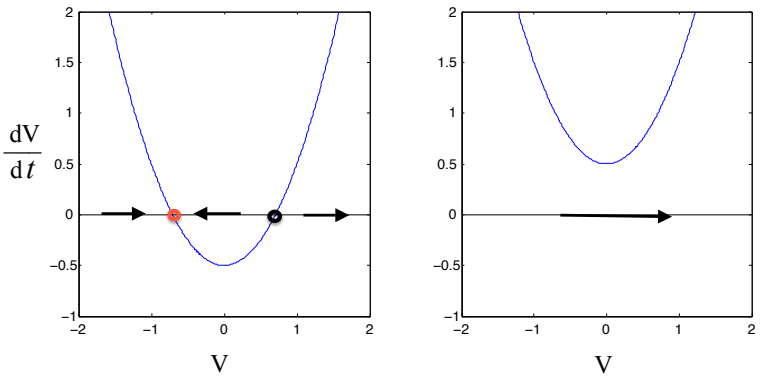


Figure 1: **Left:** The QIF neuron with subthreshold drive ($G < 0$) has two fixed points: an unstable "threshold" potential at $V^+(G)$ (black) and a stable "resting" potential at $V^-(G)$ (red). **Right:** When the drive $G$ becomes positive, the two fixed points disappear in a saddle-node bifurcation.

When $V$ is between $V^+(G)$ and $V^-(G)$, it decreases; above $V^+(G)$ or below $V^-(G)$ it increases. Thus, the positive fixed point is unstable and the negative one is stable (see Figure 1). $V^-(G)$ corresponds to a stable resting potential, while $V^+(G)$ corresponds to a threshold for spiking. If $G$ passes through zero and becomes positive, $V$ undergoes a saddle-node bifurcation and $\dot{V}$ becomes strictly positive; if $G$ is held constant at $G > 0$, $V$ spikes in finite time and both $V$ and $s$ are reset.

**Remark 3.1.1.** *If we introduce reversal potentials into our model,* (4) *becomes*

$$\begin{cases} \frac{\partial}{\partial \check{t}} V = & V^2 + (b + I(\tau \check{t}))(V_e - V) + gs(V_i - V) \\ \frac{\partial}{\partial \check{t}} s = & -\mu s \end{cases} \tag{7}$$

*When $I(\tau\check{t}) = I$ is constant, $V$ has two equilibria:*

$$V^{\pm} = \frac{b + gs + I \pm \sqrt{(b + gs + I)^2 - 4(b + I)V_e - 4gsV_i}}{2} \tag{8}$$

*The qualitative results below would also hold using these as the resting potential and threshold, though calculations based on the specific expressions for $\dot{V}$ and $V^{\pm}$ would have to be repeated using these new expressions.*

If the input current $I(\tau\check{t})$ varies on this fast time scale, then while the net current $G$ and the membrane potential $V$ are both below 0, $V$ acts like a leaky integrator for the input $I(\tau\check{t})$. As $I(\tau\check{t})$ varies, $V$ approaches $V^-(G_{\check{t}}) = -\sqrt{-b + gs - I(\tau\check{t})}$. When $G$ is roughly constant and $V$ is close

to $V^-(G)$, $\frac{\partial}{\partial \check{t}}V$ can be described by its linearization:

$$\frac{\partial}{\partial \check{t}}V \approx 2V^-(G)(V - V^-(G)) = -2\sqrt{-G}(V - V^-(G)). \tag{9}$$

This describes a membrane potential approaching its stable resting point at exponential rate $\lambda(G) = -2\sqrt{-G}$ on time scale $\check{t} = \frac{t}{\tau}$; thus, this approach is more rapid for small $\tau$ and for more negative net current $G$. When $I(\tau\check{t})$ changes, this is the approximate rate at which $V$ approaches the new value of $V^-(G)$; if $V$ is initialized near $V^-(G)$, this is the rate at which the initial conditions are "forgotten" by $V$, which can also be interpreted as the rate at which the a surplus of current leaks away. If $V$ is initialized farther from $V^-(G)$, the linear approximation of the approach rate is no longer useful, but the qualitative behavior is the same: $V$ approaches $V^-(G)$ on the $\check{t}$ time scale unless $V$ is over its spiking threshold $V^+(G)$, in which case it spikes.

This "spike-or-forget" behavior is characteristic of leaky neural integrators. It is not, however, characteristic of oscillators as they are generally modeled in theoretical literature. This behavior is possible for the NG oscillator only because two orthogonal processes are at work: a leaky integrator in the form of a QIF neuron and stably periodic oscillator in the form of an inhibitory autapse.

3.2. **The slow subsystem.** We set $\mathbf{t} = \mu\check{t}$ in (4) and let $\mu \to 0$ to describe the slow inhibition dynamics:

$$\begin{cases} \mu V' = & V^2 + G \approx 0 \\ s' = & -s \end{cases} \tag{10}$$

where $V'$ denotes $\frac{\partial}{\partial \mathbf{t}}V$. On the $\mathbf{t}$ time scale, $s$ decays, gradually increasing $G$ until it reaches zero, while $V$ is forced to obey the hard constraint $V^2 + G$ by closely tracking the stable fixed point $V^-(G)$. When $s$ passes $\frac{b}{g}$, $G$ passes zero and the two fixed points annihilate, so it is no longer possible to describe the system by its slow behavior. Instead, $V$ reaches $V_{spike}$ on the $t$ time scale as described by the fast subsystem above, and $s$ resets to 1. Then $V$ approaches $V^-(G)$ on the fast time scale until it is very close, at which point the system can again be described by its slow subsystem. This limit cycle is illustrated in Figure 2.

Let $T(\mu)$ denote the period of the limit cycle on time scale $\mathbf{t}$, as a function of $\mu$. When $\mu \to 0$, the period starts with $s_0 = 1$ and ends immediately after $G$ reaches 0, so on the slow time scale $\mathbf{t}$, the period of this limit cycle is approximately $T(0) = \ln(\frac{g}{b})$:

$$\begin{aligned} 0 \approx G_{T(\mu)} =& b - gs_{T(0)} = b - ge^{-T(0)} \\ T(0) =& \ln(\frac{g}{b}) \end{aligned} \tag{11}$$

## 4. The NG oscillator's response to pulses

*Here we prove that when the NG oscillator* (1) *receives short pulses of excitatory synaptic input, its response is to "spike-or-forget"; furthermore, if the input pulse is long compared to the timescale of*

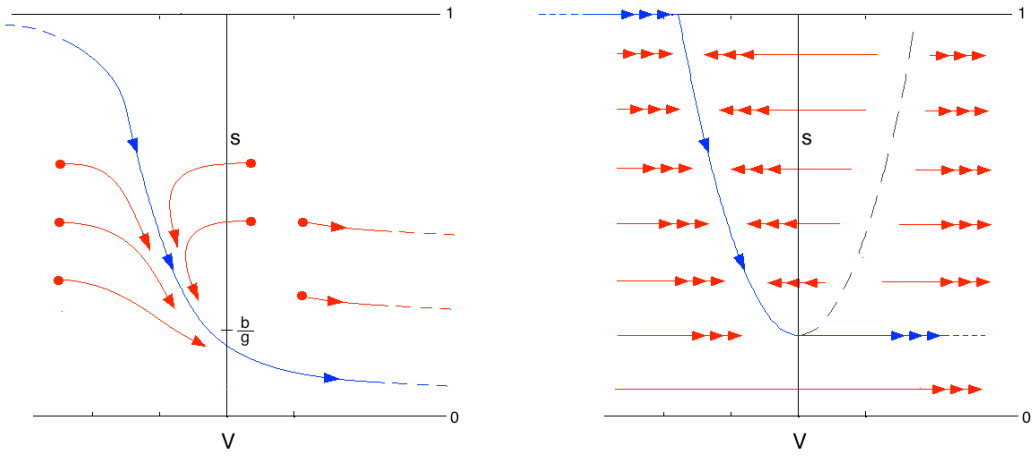


Figure 2: **Left:** The blue path is the limit cycle for (1) with $I(\cdot) = 0$, $V_{spike} = \infty$, and $V_{reset} = -\infty$. The red paths are the trajectories from various initial conditions. When any trajectory reaches a spike, it resets to $(V_{reset}, 1)$ and joins the blue limit cycle. **Right:** The blue path is the limit cycle for (1) with $I(\cdot) = 0$, $V_{spike} = \infty$, and $V_{reset} = -\infty$, as $\mu \to 0$. Just after a spike, $s = 1$, so $V$ quickly rises to $V^-(b-g) = -\sqrt{-b+g}$. It then tracks $V^-(b-gs)$ as $s$ decays slowly. When $s$ passes below $\frac{b}{g}$, $V^-$ disappears in a saddle-node bifurcation and $V$ immediately spikes. $V$ resets to $V_{reset}$ and $s$ resets to 1.

*the membrane dynamics, the NG oscillator spikes with strong preference for coherent input pulses. We show that a wide range of general oscillators do not share this behavior.*

4.1. **NG oscillator phase.** Before we can discuss phase response functions for the NG oscillator, we need to define asymptotic phase for this system. Any point $p$ on an asymptotically stable limit cycle with period $T$ may be assigned a $T$-periodic phase variable $\Theta$ such that $\dot{\Theta} = 1$. Points in the neighborhood of the limit cycle may be assigned asymptotic phases in $[0, T)$ such that initial conditions with the same asymptotic phase flow converge asymptotically on the trajectory initialized at that phase on the limit cycle [[[REF]]]. Sets of points $p$ with the same asymptotic phase are called "isochrons."

For the NG oscillator, all trajectories join the limit cycle at each spike, so initial conditions that reach spikes at the same time have the same asymptotic phase. We let $T_s(V_0, s_0, \mu)$ denote the time (on time scale $\mathbf{t}$) required to reach $V = V_{spike}$ from initial condition $(V_0, s_0)$ when the timescale separation parameter is $\mu$; we can define $\mathbf{\Theta}(V, s, \mu)$, the asymptotic phase of a point $(V, s)$ in state space with timescale separation parameter $\mu$, as

$$\mathbf{\Theta}(V_0, s_0, \mu) = T(\mu) - T_s(V_0, s_0, \mu). \tag{12}$$

For an illustration of these isochrons, see Figure 3, right. We note that $\Theta$ measures phase on the slow time scale $\mathbf{t}$. After a spike, we have $\Theta_{\mathbf{t}} = \mathbf{t}$ and $s_{\mathbf{t}} = e^{-\mathbf{t}}$; so on the limit cycle between spikes,

$$(V, s) = (V^-(b - ge^{-\Theta}), e^{-\Theta}) \qquad \Theta = \ln\left(\frac{1}{s}\right) \tag{13}$$

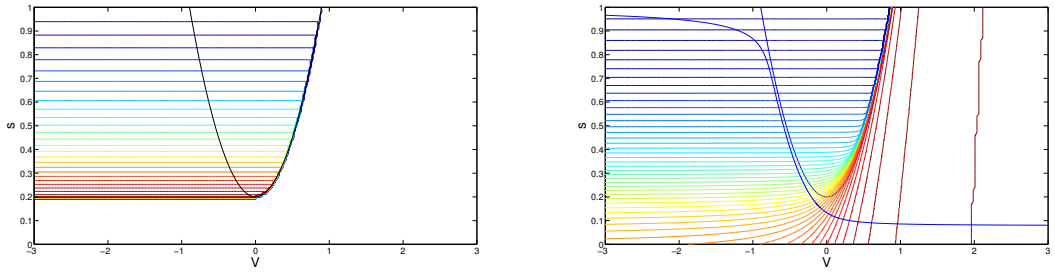


Figure 3: **Left:** Isochrons of (4) in the singular limit $\mu \to 0$. Isochrons represent a range of phases $\Theta$ from 0 (blue) to $T_0 = \ln(\frac{g}{b})$ (red). **Right:** Isochrons of (1), for $\mu$ small but nonzero. Stable limit cycle is blue. [[[REFERENCE IT]]]

4.1.1. *NG oscillator phase:* $\mu \ll 1$. If the NG oscillator is initialized at state $(V_0, s_0)$ and $\mu \ll 1$ (i.e., $\tau \ll \tau_s$), NG oscillator spikes occur as soon as $s_0$ decays to $\frac{b}{g}$, making $G > 0$, or immediately if $V_0 > V^+(G)$ or $s_0 < \frac{b}{g}$. If a spike occurs immediately, then $T_s(V_0, s_0, 0) = 0$; if not, then

$$\begin{aligned} \frac{b}{g} =& s_{T_s(V_0,s_0,0)} = s_0 e^{-T_s(V_0,s_0,0)} \\ T_s(V_0, s_0, 0) =& \ln\left(\frac{gs_0}{b}\right) \end{aligned}$$

Note that when $T_s(V_0, s_0, 0)$ is not defined when $V_0 = V^+(b - gs_0)$: from this initial state, the fast subsystem does not go to its stable equilibrium or spike, so the dynamics cannot be adequately described by the slow subsystem. From (12) and , we can write

$$\mathbf{\Theta}(V_0, s_0, \mu) \approx \begin{cases} T(0) - \ln\left(\frac{gs_0}{b}\right) = \ln\left(\frac{1}{s_0}\right) & \text{for } s_0 > \frac{b}{g} \text{ and } V_0 < V^+(b - gs) \\ T(0) & \text{for } s_0 < \frac{b}{g} \text{ or } V_0 > V^+(b - gs) \end{cases} \tag{14}$$

This function is well-defined for $V_0 \neq V^+(b - gs_0)$. We note that our assignment of phase for a singularly perturbed system follows the methodology of singularly perturbed phase response curves from [17].

For an illustration of isochrons in the singular limit, see Figure 3, left. As is evident in this image and from the fact that (14) is a function of $s_0$ but not $V_0$, the isochrons are horizontal lines. We shall refer to states above the threshold $V^+(b-gs)$ as "spiking states." Perturbations in the voltage direction do not advance the phase at all unless they carry $V$ to a spiking state. This is the isochron representation of a spike-or-forget response to perturbation.

4.2. **Short pulses.** The study of phase response curves generally focuses on two different types of pulses: infinitesimally small in magnitude, and infinitesimally short in duration. The first does not adequately illustrate the unique response of the NG oscillator to perturbation, so here we focus on the second.

If an excitatory square pulse arrives of finite duration $\delta$ (measured on in un-rescaled time $t$), then a spike may be evoked upon the arrival of the pulse, during the pulse, or afterwards. If $\delta \ll \tau_s$,

then $s$ (and hence $\Theta$) changes negligibly during the pulse; thus, if a spike occurs during the pulse, then at the end of the pulse $s \approx 1$. In slow time, this is an "instantaneous pulse." If, for a fixed $\delta \ll \tau_s$, we let $\mu \to 0$, then pulses may be treated as instantaneous, and the dynamics after a pulse are as described for $\mu \ll 1$ above: if $V < V^+(b - gs)$, $V$ goes in fast time to $V^-(b - gs)$, whereas if $V > V^+(b - gs)$, a spike occurs in fast time and then $V$ goes to $V^-(b - gs)$. In slow time, the arrival of a pulse either triggers a spike immediately or fails to advance the next spike at all.

**Remark 4.2.1.** *For simplicity, we henceforth assume that a single pulse is not strong enough to evoke a spike and then carry $V$ to a spiking state again; such a pulse would be strong enough to evoke a spike at any time, and an analysis of such forcing would not be very interesting.*

We sum up this spike-or-forget response in a theorem:

**Theorem 4.2.1.** *If system (1) is forced by an excitatory pulse $I(t)$ with support in the interval $t \in [0, \delta]$, in the limit as $\frac{\delta}{\tau_s}$ and $\mu$ go to zero, the PTC takes the form*

$$F(\Theta) = \begin{cases} \Theta & \text{if } \Theta < \hat{\Theta} \\ T(0) & \text{if } \Theta > \hat{\Theta} \end{cases} \tag{15}$$

*for some $\hat{\Theta} \in S^1 = (0, T(0)]$.*

**Remark 4.2.2.** *A pulse displaces a point on the limit cycle at phase $\hat{\Theta}$ onto the curve $V^+(b - gs)$, where the asymptotic phase is not defined, so the PTC is not well-defined for $\Theta = \hat{\Theta}$. We address this issue carefully when we prove the persistence of the phase response for nonzero $\mu$ below. At phase 0, the system is jumping instantly to $V^-(b - gs)$ so the initial state before the pulse is not well-defined; but a spike cannot be evoked before $\hat{\Theta}$, so we may set $F(0) = 0$.*

A PTC of this form is illustrated in Figure 4, top. From this theorem, we derive a corollary regarding the supremal value of the PRC, a value that will have direct implications for the oscillator's capacity to lock to periodic stimuli:

**Corollary 4.2.1.** *Let $\Delta(\Theta) = F(\Theta) - \Theta$ define the PRC of the system described above:*

$$\Delta(\Theta) = \begin{cases} 0 & \text{if } 0 < \Theta < \hat{\Theta} \\ T(0) - \Theta & \text{if } \hat{\Theta} < \Theta \leq T(0) \end{cases} \tag{16}$$

*The supremum of $\Delta$ occurs at $\Theta = \hat{\Theta}$:*

$$\sup_{\Theta \in [0, T(0))} \Delta(\Theta) = T(0) - \hat{\Theta} = \ln\left(\frac{g}{b}\right) - \hat{\Theta}. \tag{17}$$

This PRC is illustrated in Figure 4, bottom. It clearly represents the spike-or-forget behavior previously discussed. Left of $\hat{\Theta}$, the perturbation does not affect the phase at all; right of $\hat{\Theta}$, the phase is reset to a spike.

*Proof.* Let an excitatory perturbation arrive when the system is at phase $\Theta_0$ on the limit cycle. When the pulse arrives, the system is at state $(V_{\Theta_0}, s_{\Theta_0}) = (V^-(b - ge^{-\Theta_0}), e^{-\Theta_0})$. $F(\Theta_0)$ denotes the phase after the pulse; let $\tilde{V}_{\Theta_0}, s_{\Theta_0}$ denote the voltage after the pulse.

$s_{\Theta_0}$ decreases with $\Theta_0$, so $V_{\Theta_0}$ increases with $\Theta_0$. During the pulse, $\frac{\partial}{\partial t}V = -V^2 + b - gs_{\Theta_0} + I$, so at any fixed $V$, $\frac{\partial}{\partial t}V$ increases with $\Theta_0$. For larger $\Theta_0$, $V$ is larger at the beginning of the pulse and

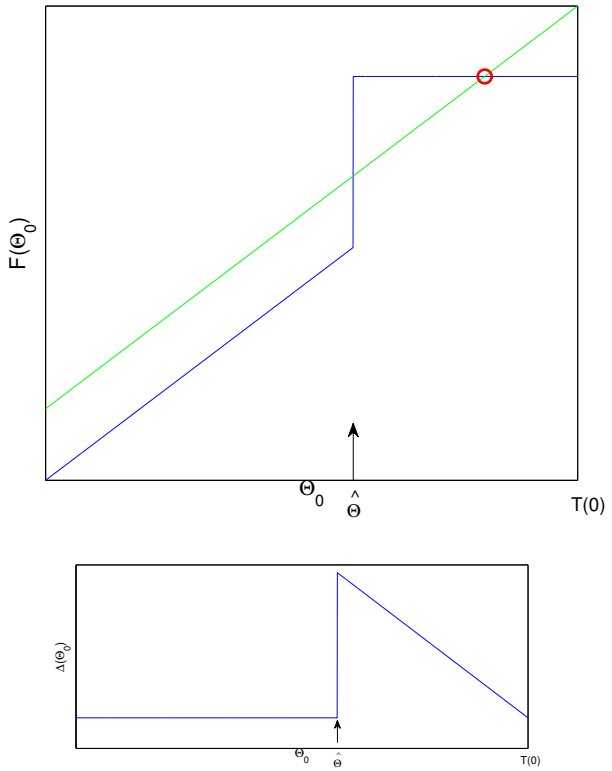


Figure 4: **Top:** The general form of the NG oscillator's PTC assuming $\mu \to 0$, as described by (15). **Bottom:** The corresponding PRC.

its derivative is everywhere larger; therefore, its value at the end of the pulse, $\tilde{V}_{\Theta_0}$, strictly increases with $\Theta_0$.

The threshold for spiking, $V^+(b - gs_{\Theta_0})$, strictly decreases with $\Theta_0$; therefore, $\tilde{V}_{\Theta_0} - V^+(b - s_{\Theta_0})$ strictly increases with $\Theta_0$. We let $\hat{\Theta}$ denote the phase $\Theta_0$ at which $\tilde{V}_{\Theta_0} - V^+(b - s_{\Theta_0})$ crosses zero. If $\Theta_0 < \hat{\Theta}$, then $\tilde{V}_{\Theta_0} < V^+(b - gs_{\Theta_0})$, and the phase defined in (14) has not changed: $F(\Theta_0) = \ln\left(\frac{1}{s_{\Theta_0}}\right) = \Theta_0$. If $\Theta_0 > \hat{\Theta}$, then $\tilde{V}_{\Theta_0} > V^+(b - gs_{\Theta_0})$ and $F(\Theta_0) = T_0$. If $\Theta_0 = \hat{\Theta}$, then $\tilde{V}_{\Theta_0} = V^+(b - gs_{\Theta_0})$, and $F(\Theta_0)$ is not defined.

□

**Remark 4.2.3.** *A similar but more complicated expression can be derived for pulses without assuming that $\delta \ll \tau_s$: in this case, $G$ may cross above zero when the pulse arrives or at some point during its duration, and these two possibilities must be treated as separate cases. A PRC associated with such a pulse is portrayed in Figure 5.*

**Remark 4.2.4.** *Spike-or-forget responses to input may occur even if cell populations participate sparsely in the rhythm. When the E-cells in a PING network receive an excitatory input, it is likely*

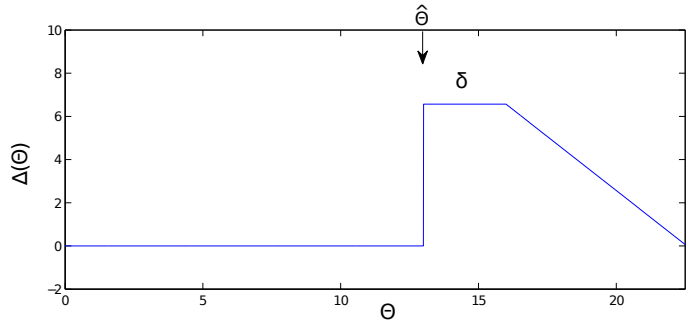


Figure 5: The PRC of the NG oscillator in response to a square pulse of length $\delta$, assuming that $\mu \ll 1$ but not that $\delta \ll \tau_s$. The plateau of duration $\frac{\delta}{\tau_s}$ (in slow time) represents phases at which a spike is evoked during the pulse rather than at its arrival. Analysis of phase locking and coupled behavior performed here may be generalized to this case. [[[FIX PICTURE?]]]

*that only a subset will respond with a spike; however, if projections from the participating E-cells "fan out" to multiple interneurons, a few E-cells may be enough to activate a full I-cell volley. This observation justifies using the NG oscillator to represent a forced PING network with sparse E-cell participation. (However, see Atallah et al 2009 [2] for evidence that interneurons are only recruited proportionally to excitatory participation.)*

4.2.1. *Limiting case: coincidence detector.* We continue to assume $\mu \to 0$ and $\delta \ll \tau_s$. Here we examine the effect of a pulse of fixed height.

**Theorem 4.2.2.** *Suppose the excitatory pulse forcing the system described in Theorem 4.2.1 attains maximal height $h$, i.e., $\sup I(t) = \sup_{0\le t\le\delta} I(t) = h$. Then $\hat{\Theta} \ge \ln(\frac{g}{h+b})$, with equality for a square pulse in the limit of large $\frac{\delta}{\tau}$.*

**Corollary 4.2.2.** *The supremum of $\Delta(\Theta)$ is less than or equal to $\ln\left(1+\frac{h}{b}\right)$, with equality for a square pulse in the limit $\delta \gg \tau$.*

**Remark 4.2.5.** *One important implication of this corollary is that a pulse of a fixed height can have maximum impact on NG oscillator phase when its duration is long compared to the membrane time constant, i.e. long enough that the membrane can reach its new resting potential during the pulse.*

**Remark 4.2.6.** *A second important implication is that to the extent that $\delta$ is large compared to $\tau$, the amount by which the pulse can shorten the NG oscillator's period is determined by pulse height.*

*Proof.* Suppose a pulse arrives when $\Theta = \Theta_0$. Since $\delta \ll \tau_s$, $s$ stays approximately constant at $s_{\Theta_0}$ during the pulse, and therefore $\Theta$ stays constant at $\Theta_0$. A spike cannot occur during the pulse unless $G \ge 0$. During the pulse, the supremum of $G$ is $b - g s_{\Theta_0} + h$, so a spike cannot occur unless

$$\begin{aligned} 0 \le & b - g s_{\Theta_0} + h \\ s_{\Theta_0} \le & \frac{h+b}{g} \end{aligned}$$

From (13),

$$\begin{aligned} e^{-\Theta_0} \leq & \frac{h+b}{g} \\ \Theta_0 \leq & \ln\left(\frac{g}{h+b}\right) \end{aligned} \tag{18}$$

Therefore we must have $\hat{\Theta} \geq \ln\left(\frac{g}{h+b}\right)$.

Suppose a square pulse of duration $\delta$ and height $h$. For any $\Theta_0 > \ln(\frac{g}{b+h})$, we have $G = b - gs_{\Theta_0} + h > 0$ during the pulse. On the fast time scale $\check{t}$, the duration of the pulse is $\frac{\delta}{\tau}$, and the derivative of $V$ is $V^2 + G$, which is bounded above zero during the pulse. So if $\frac{\delta}{\tau}$ is sufficiently long, $V$ can travel from $V^-(b - gs_{\Theta_0})$ to $V^+(b - gs_{\Theta_0})$ during the pulse, guaranteeing a spike either during or immediately after the pulse. Since a spike arriving at any $\Theta_0 > \ln(\frac{g}{b+h})$ is followed immediately by a spike, we must have $\hat{\Theta} \leq \ln(\frac{g}{h+b})$. We conclude that in this case, $\hat{\Theta} = \ln\left(\frac{g}{h+b}\right)$.

The corollary follows from 4.2.1:

$$\begin{aligned} \sup_{\Theta \in [0, T(0))} \Delta(\Theta) = & \ln\left(\frac{g}{b}\right) - \hat{\Theta} \\ \leq & \ln\left(\frac{g}{b}\right) - \ln\left(\frac{g}{h+b}\right) \\ = & \ln\left(1 + \frac{h}{b}\right) \end{aligned}$$

with equality in the limit $\frac{\delta}{\mu} \to \infty$. □

When $\frac{\delta}{\tau}$ is large, the cutoff phase $\hat{\Theta}$ is $\ln(1 + \frac{h}{b})$, a decreasing function of $h$: the higher the rate of inward current during the pulse, the earlier it can evoke a spike. Therefore, concentrating a fixed amount of charge $K$ into a short time window (increasing the maximum pulse height inversely with the duration) has a significant impact to the extent that $\delta$ remains large with respect to $\tau$, increasing the amount by which the pulse can shorten the oscillator's period. Thus, to the extent that $\frac{\delta}{\tau}$ is large, the NG oscillator acts as a powerful coincidence/coherence detector.

**Remark 4.2.7.** *It is also straightforward to show that to the extent that $\frac{\delta}{\tau}$ is small, the effect of a pulse on $V$ (and hence the value of $\hat{\Theta}$) depends on the charge $K$ carried by the pulse; in this extreme, the NG oscillator cannot act as a coincidence/coherence detector at all.*

Later we will show that if a pulse is delivered to the oscillator periodically, this range of coincidence sensitivities corresponds directly to a range of periods at which phase locking will occur.

4.3. **In Relation to Other Oscillators.** The behavior of the NG oscillator in the limit $\delta \gg \tau$ is particularly noteworthy in relation to the PRC's of phase oscillators. We consider the class of oscillators that can be written in the form

$$\dot{\phi} = 1 + g(\phi)\left(\epsilon I(t) + B\right) \tag{19}$$

where $I(\cdot) \geq 0$ is a time-varying excitatory input, $g(\cdot) \geq 0$ is a non-negative PRC, $B \geq 0$ is the level of additional excitatory drive, and $\epsilon \geq 0$. As we demonstrate in Appendix 9.1, such systems include LIF neurons, QIF neurons, and any type-1 limit-cycle oscillator if any forcing is sufficiently weak. This form represents any oscillator for which

(1) excitation advances phase, and

(2) at any phase, the contribution of excitatory input to the rate of phase advance sums linearly.

In Appendix 9.2, we show that the height of the PRC of such an oscillator is limited in terms of the charge $K$ carried by the pulse. In particular, the following inequality holds:

$$\Delta(\Theta_0) < \sqrt{-\frac{\partial T_B}{\partial B}\bigg|_{B=0}}\sqrt{K} \tag{20}$$

where $T_B$ is the period of the oscillator as a function of $B$ (when $\epsilon = 0$) and $K = \sup_{t_0 \in \mathbb{R}} \int_{t_0}^{t_0+T_0} I(t)dt$ denotes the maximal charge carried by the forcing input during one natural period of the oscillator, or in the case of a pulsatile input, the charge carried by the pulse. The term $-\frac{\partial T_B}{\partial B}\Big|_{B=0}$ expresses the sensitivity of the oscillator's period to variation in tonic drive; thus, (20) shows that the sensitivity of the oscillator's phase to input *relative to its sensitivity to tonic drive* is strictly limited by the charge carried by the input, and thus cannot be strongly influenced by input coherence.

The maximal value of the PRC represents the most a given input can shorten the oscillator's period. Inequality (20) tells us that the maximal period-shortening power of a collection of pulses cannot increase beyond a certain bound no matter how coherently those pulses arrive. By contrast, the PRC of the NG oscillator can approach a supremum of $\ln(1 + \frac{h}{b})$ when $\frac{\delta}{\tau}$ is large. As long as our previous assumption $\mu\delta \ll 1$ holds, the PRC height is independent of $\mu$, as is the NG oscillator's sensitivity to tonic drive: setting $b = b_0 + B$ in (11), we see that

$$-\frac{\partial T_B}{\partial B}\bigg|_{B=0} = \frac{1}{b_0}. \tag{21}$$

If $\frac{\delta}{\tau}$ is large, then by the theorem above, the supremum of the PRC is close to $\ln\left(1 + \frac{h}{b}\right)$; the charge carried by a pulse of fast-time-scale duration $\delta$ is $K = \delta\tau h$, so if $\tau$ is sufficiently small, a pulse of charge $K$ may be tall enough that $\ln\left(1 + \frac{h}{b}\right)$ exceeds $\sqrt{-\frac{\partial T_B}{\partial B}\Big|_{B=0}}\sqrt{K}$, and therefore the PRC reaches a height exceeding the limit imposed by equation (20).

The difference between (19) and the NG oscillator can be viewed geometrically. For (19) (and any system that can be represented as (19), including 1-dimensional model neurons and weakly forced limit cycle oscillators), excitation contributes linearly to phase advance: at a given phase, the rate of phase advance is a constant plus a linear function of the drive. A weakly forced limit cycle oscillator can be put in this form because its isochrons are locally linear, and therefore the effect of an excitatory perturbation scales linearly with its magnitude. Excitatory perturbations in an NG oscillator carry it almost perpendicularly to its limit cycle and parallel to its isochrons (see Figure **??**), so small, sustained inputs effect little phase advance; but the isochrons turn almost ninety degrees at the threshold voltage, so inputs sharp enough to force the system across this line effect a

very large phase advance. This is why it is relatively insensitive to drive but can be very sensitive to short, sharp pulses. Such a system cannot be adequately described in the form (19) because the isochrons bend sharply, i.e. the rate of phase advance is strongly nonlinear with respect to the magnitude of the input current.

The difference can also be stated in terms of leakiness. In order to evoke a spike, a pulse must carry charge to the cell population fast enough to overwhelm the leak current. If it does, a spike volley occurs; if it does not, the leak causes all effect of the pulse to be quickly forgotten. An oscillator without this property, e.g. a one-dimensional phase oscillator or an oscillating LIF or QIF neuron without an inhibitory autapse, cannot forget inputs: any input can only expedite a spike to the extent that it can advance the oscillator's phase, and phase advances are not forgotten. The NG oscillator's phase advances steadily in the $s$ direction, but inputs push it in the $V$ direction, and on short time scales $V$ has a stable fixed point, creating "leakiness" that allows inputs to be forgotten.

4.4. **In Relation to Leaky Integrators.** The NG oscillator's spike-or-forget response to pulsatile input is characteristic of a leaky integrator, such as a QIF neuron with subthreshold drive:

$$\dot{V} = \frac{1}{\tau}(V^2 + B) \tag{22}$$

where $B \leq 0$. This is, in fact, a complete description of the fast subsystem of the NG oscillator with small $\tau$. For $B < 0$, it has a stable equilibrium at $-\sqrt{-B}$ and an unstable equilibrium at $\sqrt{-B}$. When $\tau$ is small, perturbations that do not carry $V$ above $\sqrt{-B}$ are quickly forgotten as $V$ returns to $-\sqrt{-B}$, while perturbations that carry $V$ above $\sqrt{-B}$ are immediately followed by a spike. Like the NG oscillator, its response to pulses with duration long compared to $\tau$ is a function of the height of the pulse rather than the integral, so it can act as a coherence filter.

However, the leaky integrator ultimately returns to its fixed point after perturbations, and therefore cannot oscillate without input. A PRC cannot be drawn for this system: it is not an intrinsic oscillator, and therefore cannot be assigned a phase at all. When $B > 0$, the fixed points no longer exist, and the system does oscillate without additional input; however, the oscillating QIF neuron is not leaky. Any excitatory input pushes the system in the direction of the advancing phase, and therefore cannot be effectively forgotten. To prove this, we show in Appendix 9.1 that the oscillatory QIF neuron can be put in the form of equation (19) by a change of variables, in which form it is subject to the non-leaky constraint imposed by (20). Furthermore, in Appendix 9.3, we directly calculate the phase response curve of an oscillating QIF neuron in response to strong, short pulses, and find that in a phase locked state, its spikes and its forcing input pulses may not be well-aligned.

[[[FOR CTC?]]]

[[[This difference becomes especially important in the case of mutually-coupled NG oscillators, described in Section 6.]]]

## 5. Periodically Forced NG Oscillators

*Here we show that the distinctive PRC of the NG oscillator causes it to phase lock to periodic pulses at a phase optimal for CTC.*

We can use the PRCs defined above to study the NG oscillator under periodic forcing. For some forcing period $T_I$, we introduce a $T_I$-periodic forcing-phase variable $\Phi$ into (4) and write

$$\begin{cases} V' = & \frac{1}{\mu}(V^2 + G) \\ s' = & -s \\ \Phi' = & 1 \end{cases} \tag{23}$$

where

$$G = b - gs + I(\Phi)$$

and $V$ resets to $V_{reset}$ when it reaches $V_{spike}$, simultaneously resetting $s$ to 1. Now the system is autonomous. In [[[PAPER1ac]]], we find that this system produces only periodic and quasiperiodic behavior; in [[[Paper1b]]], we show that if forcing consists of square pulses, it can only phase lock with spikes occurring at only one forcing phase, i.e., it phase locks monostably. Here, we approximate its behavior by assuming, as above, that the periodic forcing is short and pulsatile, and that the system is on its stable limit cycle every time a pulse arrives, allowing us to define a PTC $F(\cdot)$ and a PRC $\Delta(\cdot)$ describing the response to each forcing pulse. When phase locking occurs, these functions can tell us the phase relationship between forcing pulses and spiking.

We let $\Theta$ denote the circular phase variable after a phase reduction, and $\bar{\Theta}$ denote a lift of this variable to $\mathbb{R}$. We have $\Theta' = 1$ between pulses, and $\bar{\Theta}$ resets to $F(\bar{\Theta})$ when pulses arrive. Pulses are separated by time $T_I$, so if a pulse arrives when the system is at phase $\bar{\Theta}_0$, the next pulse will arrive at phase $\bar{\Theta}_1 = F(\bar{\Theta}_0) + T_I$. 1:1 phase-locking occurs if $\bar{\Theta}_1 = \bar{\Theta}_0 + T(\mu)$ such that the NG oscillator is returning to phase $\Theta_0$ for the first time just when the next pulse arrives. So phase-locking occurs if

$$\bar{\Theta}_0 + T(\mu) = F(\bar{\Theta}_0) + T_I = \Delta(\bar{\Theta}_0) + \bar{\Theta}_0 + T_I \tag{24}$$

$$F(\bar{\Theta}_0) = \bar{\Theta}_0 + T(\mu) - T_I \tag{25}$$

or, equivalently, if

$$\Delta(\bar{\Theta}_0) = T(\mu) - T_I. \tag{26}$$

From the study of iterated dynamical systems, we recall that phase-locking is stable if the slope of the updating function at the intersection with the diagonal has magnitude less than one, i.e. if

$$-2 < \Delta'(\bar{\Theta}_0) < 0 \tag{27}$$

5.1. **Small $\mu$ and $\frac{\delta}{\tau_s}$.** As discussed earlier, when $\mu \ll 1$ and $\frac{\delta}{\tau_s} \ll 1$, we have a PTC of the form (15). (As discussed in Section 7, this form is qualitatively accurate for a wide range of parameters.)

Phase-locking is possible when a line at height $T(0) - T_I$ intersects the phase-response curve; since $\Delta(\Theta)$ reaches a minimum of 0 and a maximum of $\Delta(\hat{\Theta})$ (where $\Delta(\hat{\Theta})$ is calculated in the right-hand limit), such an intersection occurs if and only if

$$0 \leq T(0) - T_I \leq \Delta(\hat{\Theta}). \tag{28}$$

This intersection is transverse when inequalities are strict. Examining (16) and Figure 6, we see that when $T(0) - T_I$ intersects $\Delta(\cdot)$ transversely, one intersection occurs in the interval $(\hat{\Theta}, T(0))$.

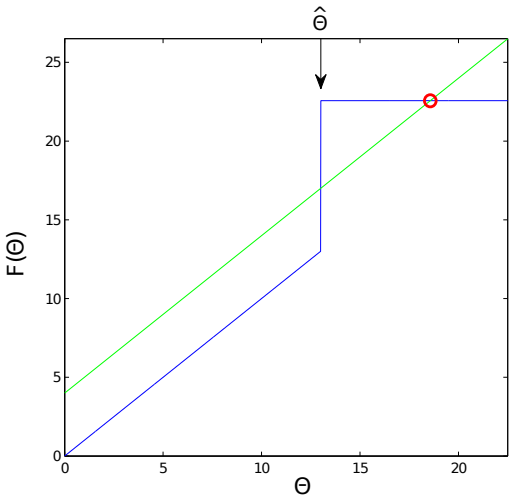


Figure 6: The PTC described by (15) intersects the diagonal $\bar{\Theta}_0+T(0)-T_I$ once with slope zero, representing a stable phase locking phase. When the NG oscillator is locked to pulses at this phase, pulses reset the oscillator to phase $T(0)$, and a spike occurs immediately.

Since $\Delta'(\Theta_0) = -1$, we can see from (27) that this intersection corresponds to a stable phase lock. This intersection corresponds to a pulse arriving near the end of the natural gamma period and immediately evoking a spike, resetting the oscillators phase to $T(0)$. The phase-lock represented by this intersection is stable. The other intersection occurs at the cutoff phase $\hat{\Theta}$ as $\Delta(\Theta)$ jumps discontinuously from 0 to its maximum; the slope here is infinite, so this phase-lock cannot be stable.

Our PRC demonstrates that for a range of forcing periods $T_I < T(0)$, stable phase-locking occurs and is characterized by pulses arriving and immediately evoking spikes. In addition to this qualitative description, we can use Theorem 4.2.2 to quantitatively describe when stable phase locking will occur. This theorem shows that for pulses long relative to $\mu$, $\hat{\Theta}$ is mainly determined by the pulse height and therefore very sensitive to input coherence. So for pulses long relative to $\mu$, this oscillator not only serves as a coincidence/coherence "detector," but also as a coincidence/coherence "phase-locking filter": a periodic forcing pulse that is a sum of small periodic pulses phase locks the oscillator at a broader range of forcing frequencies if the smaller pulses arrive close to the same forcing phase, i.e. if they arrive more coherently. In the limit of large $\frac{\delta}{\tau}$, $\sup \Delta(\hat{\Theta}) = \ln\left(1+\frac{h}{b}\right)$, so from (28), stable phase locking occurs if and only if $T(0) - \ln\left(1+\frac{h}{b}\right) < T_I < T(0)$.

The cutoff phase $\hat{\Theta}$ determines the range of forcing periods at which a particular pulse can phase-lock the gamma rhythm. When such a phase lock does occur, the oscillator spikes just after the arrival of the pulse. Equivalently, the pulse arrives when inhibition $s$ is at its lowest point in the oscillator's phase locked period. This arrangement is ideal for CTC: if the forcing phase of the pulse corresponds with the arrival of information (e.g. via a labeled-lines code), then this information arrives when the local network is the least inhibited and therefore the most responsive to excitatory input. A single pulse arriving at a random time during the oscillator's period is unlikely to arrive at such an optimal moment, and therefore the effect of the pulse is more likely to be shunted out by

inhibition. Thus, an information-carrying pulse arriving periodically at such a period and with such an amplitude and coherence that it can phase lock the oscillator achieves a significant advantage over other inputs at conveying its information by evoking a local spiking response.

[[[MOVE?]]]

**Remark 5.1.1.** *The PRCs measured by Akam et al [1] pictured in Figure 12 and discussed in Remark 7.1 both advance and delay phases, and therefore may lock stably to periodic pulses both faster and slower than the natural frequency of the network. In the case of the PRC in response to stimulating the alveus, this fixed point corresponds to pulses arriving just before the phase of maximal excitatory activity, when inhibition is presumably at a minimum; in the case of the PRC in response to stimulation of the dentate gyrus, it is somewhat earlier.*

5.2. **In Relation to Other Oscillators.** As discussed in the previous section, the NG oscillator is distinguished from other oscillators by its capacity to respond preferentially to coherent input. In the previous section, we showed that PRC height is more sensitivity to coherence (relative to its sensitivity to tonic drive) than any oscillator with linear isochrons, including weakly forced oscillators and QIF and LIF neurons. In this section, we can see that PRC height corresponds to the range of forcing periods that can evoke phase locking, and therefore this range is also more sensitively dependent on coherence than that of oscillators with linear isochrons.

We have identified one other respect in which the NG oscillator distinguishes itself from the generic model oscillator. When an oscillator of the general form (19) phase locks to a pulse, the pulse arrives at a phase determined by the phase response curve $g$, which may be rotated to create an oscillator with any preferred locking phase.

Even spiking oscillators may lock to pulses at a wide range of phases. In appendix 9.3 we take as an example the QIF neuron without an autapse, under superthreshold drive:

$$\tau \dot{V} = V^2 + B + I(t) \tag{29}$$

where $B > 0$ is a baseline tonic drive that makes the neuron an oscillator and $V$ resets to $V_R$ after spikes. The PTC of this system in response to short pulses is shown in Figure **??**. When driven with period slightly shorter than its natural period, this system phase locks with pulses arriving during the first half of the interspike interval. If spikes from this neuron inhibited a local network, pulses would arrive while inhibition was still high, actively opposing CTC.

By contrast, the NG oscillator (to the extent that $\mu < 1$) only phase locks with pulses arriving immediately before its spikes. As shown above, this additional structure is ideally suited to CTC.

## 6. Coupled NG Oscillators

The PRC shape associated with an NG oscillator with small $\mu$, which we characterize and explain above, can be used to predict the behavior of two such oscillators with mutual coupling. The general case of two mutually pulse-coupled oscillators has been studied extensively in [[[PLENTY REFS]]]. The stable configurations of such a system can be studied by constructing a one-dimensional map

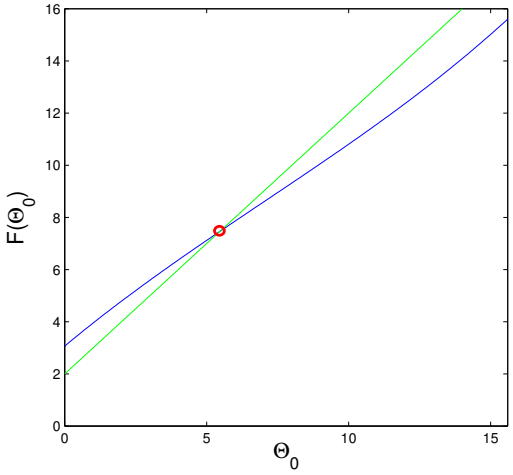


Figure 7: A QIF neuron subjected to periodic pulsatile forcing may not phase lock with spikes occurring immediately after pulses, as indicated by this PTC. Excitatory input advances its phase, but a periodic pulse can phase lock to arrive in the first half of its period. For details, see appendix 9.3.

out of the PRCs of the two oscillators. We also offer an intuitive explanation of the resulting stable dynamics.

In this section, we assume that our generic NG oscillator represents a PING process (see 2.3) such that when one reaches a spike, it can send an excitatory pulse to the other. We let $A$ and $B$ denote two such PING circuits with natural periods $T^A < T^B$. We assume that when $A$ spikes, the excitatory cell in the circuit issues an excitatory pulse to the excitatory cell in circuit $B$, which instantly adjusts its phase according to a phase response curve $\Delta^B$ (and vice versa for pulses from $B$ to $A$). We assume that both phase response curves are of form (**??**), with positive cutoff phases $\hat{\Theta}^A$ and $\hat{\Theta}^B$.

Let $\Theta_0^B$ denote the phase of oscillator $B$ at some time just before $A$ spikes at $\Theta^A = 0$, and let $\Theta_1^B$ denote its phase just before the next time $\Theta^A = 0$.

**Theorem 6.0.1.** *If $\hat{\Theta}_B < T_A$, stable phase locking occurs with pulses from $A$ immediately preceding pulses from $B$. If $\hat{\Theta}_B > T_A$, no stable 1:1 phase locking occurs.*

*Proof.* When $\Theta^A$ first reaches 0, $\Theta^B$ is immediately reset to $\Theta_0^B + \Delta^B(\Theta_0^B)$.

- If $\Theta_0^B > \hat{\Theta}^B$, $B$ immediately spikes. This spike occurs while $A$ is still at phase $0 < \hat{\Theta}^A$, so it has no effect on the phase of $A$. Now both oscillators are at zero phase. Since $T^A < T^B$, $A$ reaches a spike first after time $T^A$, at which point $\Theta_1^B = T^A$.
- If $\Theta_0^B < \hat{\Theta}^B$, the phase of $B$ is not affected by the pulse from $A$.
  - If $T^B - \Theta_0^B > T^A$, then $A$ spikes next, at which point $B$ is at phase $\Theta_1^B = \Theta_0^B + T_A$.
  - If $T^B - \Theta_0^B < T^A$, then $B$ spikes next, at which point $A$ has reached phase $T^B - \Theta_0^B$.

* If $T^B - \Theta_0^B > \hat{\Theta}^A$, then $A$ spikes immediately while $B$ is still at phase $\Theta_1^B = 0$.
* If $T^B - \Theta_0^B < \hat{\Theta}^A$, then the phase of $A$ is not affected, and $A$ spikes next when $B$ has reached phase $\Theta_1^B = T^A - (T^B - \Theta_0^B)$.

Collecting all of these conditions together, we define the map $\mathbf{F}$ from $\Theta_0^B$ to $\Theta_1^B$, illustrated in Figure 6:

$$\Theta_1^B = \mathbf{F}(\Theta_0^B) = \begin{cases} \text{(Region 1): } \Theta_0^B + T^A & \text{if } \Theta_0^B < \hat{\Theta}^B \text{ and } \Theta_0^B < T^B - T^A \\ \text{(Region 2): } 0 & \text{if } \Theta_0^B < \hat{\Theta}^B \text{ and } T^B - T^A < \Theta_0^B < T^B - \hat{\Theta}^A \\ \text{(Region 3): } \Theta_0^B + T^A - T^B & \text{if } T^B - \hat{\Theta}^A < \Theta_0^B < \hat{\Theta}^B \\ \text{(Region 4): } T^A & \text{if } \Theta_0^B > \hat{\Theta}^B \end{cases} \tag{30}$$

Fixed points of this map occur when $\mathbf{F}(\Theta_0^B) = \Theta_0^B$, i.e. the graph of $\mathbf{F}$ crosses the diagonal line $\Theta_0^B = \Theta_1^B$. Stable fixed points correspond to crossings with slope in the interval $(-1, 1)$; therefore, these cannot include crossings by discontinuous jump, so we look instead for crossings within a piecewise-continuous region. In region 1 of this map, such an intersection would imply $T_A = 0$; similarly, in region 3 such an intersection cannot occur unless $T_A = T_B$, violating our assumption of $T_B > T_A$. In region 2, such an intersection would necessitate that $\Theta_0^B = 0$, but in this interval we have $T^B - T^A < \Theta_0^B$ so $\Theta_0^B$ cannot equal zero. Therefore, if there exists a stable fixed point, it must occur region 4. If $\hat{\Theta}_B > T_A$, there is no such intersection. Otherwise, such an intersection does occur: $\Theta^B = T^A$ whenever $A$ spikes, immediately evoking a spike from $B$. We can show region-by-region that when such a stable fixed point exists, it attracts all initial conditions: region 4 maps immediately to the fixed point, regions 1 and 2 map directly into region 4, and any initial condition in region 3 eventually reaches one of the other regions.

When the system has reached this fixed point, pulses from $A$ arrive time $T^A$ after the most recent $B$ spike. □

At this stable fixed point, pulses from $A$ immediately cause $B$ to spike and reset its inhibition, so these pulses arrive when $B$ is under its lowest level of inhibition in the phase-locked cycle, an optimal arrangement for CTC from $A$ to $B$ as described earlier. However, pulses from $B$ arrive at $A$ immediately after $A$ spikes, so they arrive when $A$ is under maximal inhibition. This arrangement is perfectly *sub*optimal for CTC from $B$ to $A$. The effect is a forced directionality of communication: $A$ can evoke responses in the network local to $B$ much more easily than the feedback from $B$ can evoke responses in the network local to $A$. This process is illustrated in Figure 6.

Directed CTC arises entirely from the condition that $T_A < T_B$ (as long as the additional condition $\hat{\Theta}_B < T_A$ is met). From (11), the natural period of each oscillator is $\ln\left(\frac{g}{b}\right)$, so either period can be decreased by adding to the local tonic drive $b$ or increased by adding to the maximal inhibitory conductance $g$. If these two factors vary slowly during network interaction, $T^A$ and $T^B$ may cross each other, reversing the direction of effective CTC. In other words, the CTC that occurs between these coupled systems can be *dynamically directed*: changing local parameters changes the stable phase alignment between the oscillators, which in turn changes which oscillator's pulses arrive under heavier inhibition.

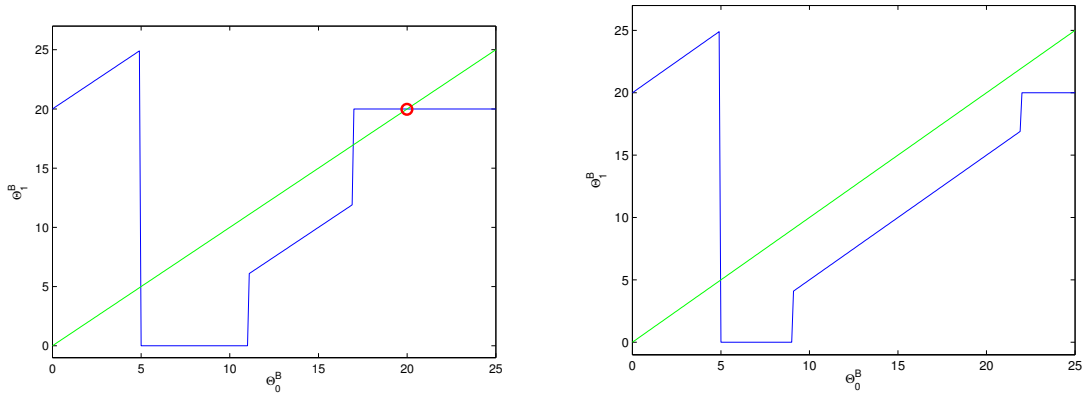


Figure 8: The map $\mathbf{F}$ from $\Theta_0^B$ (the phase of oscillator $B$ when $A$ spikes) to $\Theta_1^B$ (the phase of $B$ at the next $A$ spike). **Left:** $\hat{\Theta}_B < T_A$, so a stable fixed point exists (red). **Left:** $\hat{\Theta}_B > T_A$, so no stable fixed point exists.

Such directed communication could continue even if oscillator $B$ received subthreshold drive and could not intrinsically oscillate: $A$ could still evoke $B$ spikes at every pulse. Though $T^B$ would not be well-defined in this case, $\hat{\Theta}$ could still be interpreted as the amount of time after a $B$ spike at which $A$ pulses can first evoke another spike, and could be assigned a definite value.

Preliminary computational results suggest that the phase alignment of $A$ and $B$ and the resulting directed CTC are robust to short transmission delays, non-infinitesimal timescale separations $\mu$, and other variations in parameters. Here we only treat the simplest case; a more formal investigation of the limits of directed CTC is left for future work.

6.1. **In relation to other oscillators.** It is by no means trivial that two NG oscillators phase lock with spikes of the faster immediately preceding spikes of the slower. Van Vreeswijk [20] demonstrated that two identical oscillators of the form (19) coupled by excitatory pulses go from stable anti-synchrony to bistable "partial synchrony" (either oscillator leading the other) as the coupling strength increases. Only for very strong coupling does near-synchronous firing become stable. By a continuity argument, it should be possible to make one oscillator marginally faster than the other without qualitatively changing these results.

Our results in this section depend critically on the specific properties of the gamma-generating mechanism. One essential mechanism is the separation of time scales of membrane dynamics and inhibitory decay that allows ING and PING to forget inputs that fail to evoke immediate spike volleys. In one sense, the reason that pulses lead spike volleys in a phase-locked state is that a pulse that is not immediately followed by a spike volley fails to affect the time of the next spike volley, and so cannot create a phase lock.

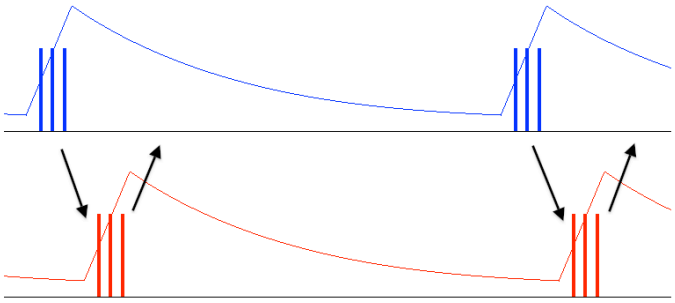

Figure 9: The characteristic phase alignment of a PING population (red) receiving periodic forcing pulses from another PING population (blue). Thick lines represent spikes; thin lines represent the level of local inhibition; downward arrows represent excitatory pulses from the sending to the receiving population and upward arrows represent feedback pulses. When the sending population produces a spike volley, the receiving population is under little inhibition and responds quickly with its own spike volley. If this second volley produces a feedback signal that returns to the sending population, it arrives under high inhibition and is ignored.

## 7. Persistence of the phase response

*Here we show analytically and computationally that the phase response curves described above in the limit $\mu \to 0$ also persist for sufficiently small $\mu > 0$.*

**Theorem 7.0.1.** *Let (4) be forced by a short pulse such that the PTC $F(\Theta)$ takes the form described in Theorem 4.2.1 with $\hat{\Theta} < T(0)$. Let $F_\mu(\Theta)$ denote its PTC for a given time scale separation $\mu > 0$. Let $D_\mu(\Theta)$ denote the diagonal line*

$$D_\mu(\Theta) = \Theta + q_\mu$$

*where $q_\mu$ is some continuous function of $\mu$. If $q_0 \in (0, T(0) - \hat{\Theta})$, there exists $\mu^* \geq 0$ such that for $\mu \in [0, \mu^*]$, $D_\mu(\Theta)$ intersects $F_\mu(\Theta)$ only twice: once in a $\mu$-small neighborhood of $\hat{\Theta}$ where $F'_\mu(\Theta) > 1$, and once at some $\Theta > \hat{\Theta}$ such that $|F_\mu(\Theta) - T(\mu)|$ and $|F'_\mu(\Theta)|$ are both $\mu$-small.*

*If $q_0 > T(0) - \hat{\Theta}$ or $q_0 < 0$, there exists $\mu^* \geq 0$ such that for $\mu \in [0, \mu^*]$, no intersection between $D_\mu(\Theta)$ and $F_\mu(\Theta)$ occurs.*

A proof is provided in Appendix 9.4.

**Remark 7.0.1.** *This theorem shows that the phase-locking properties of the PRC determined for limiting cases of time scale separation persist when the separation of time scales is more modest. In particular,*

- *The PRC height is approximately $T(0) - \hat{\Theta}$, and therefore its dependence on $h$ when $\frac{\delta}{\tau}$ is large is approximated by the theorem and corollary provided above.*

- *Under periodic pulsatile forcing, intersections of $F_\mu$ and $D_\mu$ for $q_\mu = T(\mu) - T_I$ represent phases supportive of phase locking with a pulse at period $T_I$, and the slope of $F_\mu$ at the intersection determines stability; so for small $\mu$, phase locking still only occurs with pulses arriving immediately before spikes.*

- *When two NG oscillators are coupled, the map from the phase of one oscillator at the other's spike to its phase at the next spike is a composition of these phase transition curves as described in the previous section, and phase locked states correspond to intersections of this map with the diagonal $D_\mu(\Theta)$ for $q_\mu = 0$; therefore, for small $\mu$, these oscillators still phase lock with spikes from the faster leading those of the slower.*

### 7.1. **Persistence of results into biophyically-based parameter regimes.** [[[FIX THIS JUNK]]]

Of course, in a more biophysically realistic model, $\mu$ and $\frac{\delta}{\tau_s}$ might not be singularly small. Furthermore, pulse-like inputs to neurons generally take the form of fast-rising, slower-decaying EPSCs rather than square pulses.

We claim that the analysis of the extreme cases above – $\delta \ll \mu \ll 1$ and $\mu \ll \delta \ll 1$ – capture the important qualities of the phase response curve even when the time constants are not widely separated and for non-square pulses. In particular, [[[DETAILS]]]

[[[SIMULATION RESULTS]]]

Given these results, we can draw on the results from the previous section to reason about coincidence detection in this more general case. Those results point towards an informal general rule: to the extent that $\mu < \delta$, where $\delta$ is a measure of the temporal spread of an input pulse, the NG oscillator and the circuits it may represent can act as coincidence detectors, responding preferentially when pulses arrive within a short timeframe. We may also refer to this behavior as "coherence detection": non-square pulses need not coincide perfectly to sum to a taller pulse, but may do so to the extent that they arrive coherently with each other.

[[[should this next one be moved?]]]

**Remark 7.1.1.** *Akam et al. [1] experimentally measure the PRC of gamma rhythms in the hippocampus by direct electrical stimulation and by optogenetic stimulation. The phase response curves they produce (shown in Appendix 9.5, Figure 12) bear some similarities to and some differences from those discussed here. In particular, they note phases at which their stimuli delay the onset of the trough corresponding to maximal excitatory activity. They explain the shape of their curves using a Wilson-Cowan model in which pulses are delivered mainly to the inhibitory population. In Appendix 9.5, we show that their model produces spike-or-forget results very similar to ours if the input is assumed to be entirely excitatory. Ours, however, also lends itself well to intuitive and analytical descriptions of the dependence on parameters of the PRC, and hence of phase-locking properties and coupled dynamics.*

## 8. Discussion

In this manuscript, we have shown that the network mechanism implicated in gamma oscillations has special phase-locking properties when the time scales of membrane dynamics and inhibitory decay are separated.

First, it phase locks to pulses by aligning them to the phase of the gamma oscillation with the lowest possible level of inhibition. Since these pulses presumably also encode information and local cells can only transmit or process this information to the extent that they are disinhibited, this specific phase relationship is optimal for communication between the pulse sender and the local network.

Second, if two gamma-rhythmic networks are coupled E-to-E, this mechanism creates phase locking in which pulses from the faster to the slower network arrive at minimal inhibition, while pulses from the slower to the faster arrive at maximal inhibition. This arrangement is optimized for directed CTC from the faster to the slower network.

Third, to the extent that pulses are long relative to the timescale of membrane dynamics, this mechanism acts as a "phase locking coherence filter": it can phase lock to a wider range of periods if the charge carried by a pulse arrives more coherently.

We have also shown that none of these properties are generic to phase oscillators. In particular, coherence filtering is strictly limited in a wide class of phase oscillators, and a general phase oscillator (even a spiking phase oscillator) may lock to forcing or a mutually coupled oscillator at any phase alignment, depending on the specific properties of the phase response curve.

### 8.1. Related work.

Borgers and Kopell [5] also examine the phase-locking properties of gamma-generating circuits, focusing in particular on their selectivity for coherent forcing pulses over less coherent ones. Gielen et al. [11] further study this coherence-selective phase locking in PING, as well as several simpler models including the LIF and QIF neurons. Their analyses focus on the case in which two periodic signals compete for phase-locking and are based on numerical observation backed by analytical argument; our analysis focuses on a single periodic signal and is proof-based. We also note that Gielen et al. treat their LIF and QIF neurons in their excitable rather than their oscillatory states.

Akam et al. [1] experimentally measure the phase response curves of gamma rhythms and provide a Wilson-Cowan model explanation of the curves they measure. In Appendix 9.5, we discuss the relationship between their work and ours; in particular, we point our that our phase response curves may considered a special case of theirs in which forcing is excitatory to excitatory cells. Our simpler analysis offers more intuition for this case, and allows us to study the effect of coherent input on phase locking.

Models similar to our NG mechanism model have been studied in other works. Gutkin et. al **[Gutkin2005]** numerically computed an infinitesimal phase response curve for a QIF-equivalent neuron with a decaying slow current similar to the inhibition modeled here, and Kilpatrick and Ermentrout [15] analytically described this PRC. These papers find a rightward-skewed PRC fairly similar in shape to ours. Unlike this curve, the PRCs discussed here directly describe the effects

of strong excitatory perturbations, and therefore describe what we believe is a more biophysically-relevant forcing regime. In the context of strong forcing, we provide a different way of understanding the rightward-skew of the PRC, and examine the nonlinear relationship between the stimulus strength and the PRC height. Shlizerman and Holmes [18] study the "RQIF" model, a QIF neuron with a slow recovery variable. Their model spans a wider range of dynamics than ours, but they do not address the behavior of the model under forcing and therefore have nothing to say about phase locking.

8.2. **Implications.** We propose here that the NG mechanism is ideally suited for communication through coherence (CTC): when coupled to a source of sufficiently strong or coherent pulses, it aligns its phase such that pulses arrive under less inhibition than any other input. Thus, gamma rhythms and other oscillations generated by similar mechanisms do not need any additional structure to be recruited as coherence-sensitive receivers: a source of strong pulses at an appropriate period is sufficient to established a preferred frequency and phase of communication. Bidirectionally-coupled NG mechanisms need nothing more than an imbalance of drive (established, e.g., by salient input) to engage in CTC in which the more driven oscillator sends to the less driven one and filters out feedback. Given the simplicity of the NG mechanism and the extreme ease of recruiting it for CTC, we believe that it is likely that the brain uses this mechanism to established temporary channels of selective communication between local networks.

## 9. Appendix

9.1. **Appendix: LIF and QIF neurons are type-1 forced phase oscillators.** Type-1 forced phase oscillators include any type-1 limit-cycle oscillator under weak forcing and the oscillatory states of the forced LIF neuron and the theta neuron/QIF neuron. The two models and reductions to the form of (19) are:

- **LIF:** $\tau\dot{V} = -V + B + R(b + \epsilon I(t))$, resetting from $V = 1$ to $V = 0$, with $B > 1$.

  Setting $\phi(V) = \int_0^V \frac{\tau}{-v+B} dv$, we can express this differential equation as

  $$\dot{\phi} = 1 + \frac{\tau R}{-V + B}(b + \epsilon I(t)).$$

- **QIF:** $\tau\dot{V} = V^2 + B + R(b + I(t))$, resetting from $V = V_S$ to $V = V_R$, with $B > 0$.

  Setting $\phi(V) = \int_{V_R}^V \frac{\tau}{v^2} dv$, we can express this differential equation as

  $$\dot{\phi} = 1 + \frac{\tau R}{V^2 + B}(b + \epsilon I(t))$$

The argument in the next appendix applies to these oscillator models.

9.2. **Appendix: bounds on the PRC of type-1 forced phase oscillators.** Here we determine the sensitivity of the period of a forced oscillator to variations in tonic drive and use it to put a upper and lower bounds on the phase response to a specific non-weak input $I(t)$. We work with the phase oscillator

$$\dot{\Theta} = 1 + g(\Theta)(b + \epsilon I(t)) \tag{31}$$

where $\Theta$ is a phase variable in $S^1$. We assume that this oscillator is Type-1, or in other words, $g(\Theta) \geq 0$, and that the forcing is excitatory, i.e. $I(t) \geq 0$.

We now write expressions for the sensitivity of the natural period to drive and the width of the stable phase-locking tongue, and derive a relationship between them. Let $T_0$ be the natural period of $\Theta$ with $\epsilon = 0$ and $b = 0$.

Let $\Theta_t$ be the flow of the system (31) after a spike (i.e. $\Theta = 0$) at time $t_0$. We define $T(\epsilon, b, t_0)$ as the time from $t = t_0$ to the next spike as a function of $\epsilon$, $b$, and $t_0$. We define $T_0$ as the natural period of the phase oscillator with $b = 0$ and $\epsilon = 0$. As $t$ goes from $t_0$ to $t_0 + T(\epsilon, b)$, $\Theta_t$ goes monotonically and differentiably from 0 to $T_0$. So $\Theta_t$ is invertible and differentiable with respect to $t$. We use this information to change variables from $t$ to $\Theta$:

$$\begin{aligned} T(\epsilon, b, t_0) &= \int_{t_0}^{t_0+T(\epsilon,b,t_0)} dt = \int_0^{T_0} \left(\frac{d}{dt}\Theta_t\right)^{-1} d\Theta \\ &= \int_0^{T_0} \frac{1}{1 + g(\Theta)(b + \epsilon I_{T_I}(t_\Theta))} d\Theta \end{aligned} \tag{32}$$

where $t_\Theta$ is the inverse of $\Theta_t$ with respect to $t$, i.e. the time it takes to reach phase $\Theta$ from phase 0.

We use (32) to compute $-\left.\frac{\partial T(0,b,t_0)}{\partial b}\right|_{b=0}$:

$$\begin{aligned} -\left.\frac{\partial T(0,b,t_0)}{\partial b}\right|_{b=0} &= -\left.\frac{\partial}{\partial b}\right|_{b=0} \int_0^{T_0} \frac{1}{1 + g(\Theta)b} d\Theta \\ &= \int_0^{T_0} \frac{g(\Theta)}{(1 + g(\Theta)b)^2} d\Theta|_{b=0} \\ &= \int_0^{T_0} g(\Theta) d\Theta \end{aligned} \tag{33}$$

We seek to put an upper bound on $T_0 - T(1, 0, t_0)$ (the period-shortening caused by phase advance due to $I(\cdot)$) in terms $-\frac{\partial T(b)}{\partial b}|_{b=0}$ and the charge carried by $I(t)$ during the interval $t \in (t_0, t_0 + T_0)$.

To determine an upper bound on the width of the 1:1 stable phase-locking tongue at $\epsilon > 0$, we find an upper bound for the difference between the natural oscillator period $T$ and the interspike interval under forcing, $T(1, 0, t_0)$. For a given $\epsilon$, phase-locking (stable or unstable) cannot be induced at forcing periods $T_I$ that do not allow the forcing to reduce the interspike interval to $T_I$, i.e., $T_I$ such that

$$T_0 - T(1, 0, t_0) = \int_0^{T_0} d\Theta - \int_0^{T(1,0,t_0)} dt$$

We change variables from $\Theta$ to $t$:

$$= \int_{t_0}^{t_0+T(1,0,t_0)} \frac{d\Theta}{dt} dt - \int_{t_0}^{t_0+T(1,0,t_0)} dt$$

Substituting the derivative $\dot{\Theta} = 1 + \epsilon g(\Theta_t) I(t)$ with $\epsilon = 1$ from (31),

$$\begin{aligned} &= \int_{t_0}^{t_0+T(1,0,t_0)} \left[1 + g(\Theta_t) I(t)\right] dt - \int_{t_0}^{t_0+T(1,0,t_0)} dt \\ &= \int_{t_0}^{t_0+T(1,0,t_0)} g(\Theta_t) I(t) dt \end{aligned} \tag{34}$$

To find an upper bound on $T_0 - T(1,0)$, we note that $\langle f_1(t), f_2(t) \rangle < \int_0^{T(1,0)} f_1(t) f_2(t) dt$ defines an inner product on nonnegative $f_1$ and $f_2$. Using this definition and the fact that $I(t) > 0$, we change (34) to

$$= \langle g(\Theta_t) \sqrt{I(t)}, \sqrt{I(t)} \rangle \tag{35}$$

We use the Cauchy-Schwarz inequality to bound the inner product in (35):

$$\begin{aligned} T_0 - T(1,0) \leq & \|g(\Theta_t) \sqrt{I(t)}\|_2 \|\sqrt{I(t)}\|_2 \\ = & \sqrt{\int_{t_0}^{t_0+T(1,0,t_0)} g(\Theta_t)^2 I(t) dt} \sqrt{\int_{t_0}^{t_0+T(1,0,t_0)} I(t) dt} \end{aligned} \tag{36}$$

We change variables in (36) using $\frac{d}{dt}\Theta_t = 1 + g(\Theta) I(t)$, and let $t_\Theta$ be the inverse of $\Theta_t$ with respect to $t$ as before:

$$\begin{aligned} = & \sqrt{\int_0^{T_0} g(\Theta)^2 I(t_\Theta) \left(\frac{d}{dt}\Theta_t\right)^{-1} d\Theta} \sqrt{\int_{t_0}^{t_0+T(1,0,t_0)} I(t) dt} \\ = & \sqrt{\int_0^{T_0} \frac{g(\Theta)^2 I(t_\Theta)}{1 + g(\Theta) I(t_\Theta)} d\Theta} \sqrt{\int_{t_0}^{t_0+T(1,0,t_0)} I(t) dt} \end{aligned}$$

Since the numerator under the first square root is positive and the denominator is greater than or equal to 1, the right side gets bigger when we remove 1 from the denominator. (If $g(\Theta) = 0$, this makes the denominator infinite, but the limit of this integral as $g(\Theta) \to 0^+$ still exists due to the $g(\Theta)^2$ in the numerator.)

$$\begin{aligned} T_0 - T(1,0) < & \sqrt{\int_0^{T_0} \frac{g(\Theta)^2 I(t_\Theta)}{g(\Theta) I(t_\Theta)} d\Theta} \sqrt{\int_{t_0}^{t_0+T(1,0,t_0)} I(t) dt} \\ = & \sqrt{\int_0^{T_0} g(\Theta) d\Theta} \sqrt{\int_{t_0}^{t_0+T(1,0,t_0)} I(t) dt} \end{aligned}$$

Substituting from (33):

$$= \sqrt{-\frac{\partial T(b)}{\partial b}\Big|_{b=0}} \sqrt{\int_{t_0}^{t_0+T(1,0,t_0)} I(t) dt}$$

$T(1,0,t_0)$ cannot exceed $T_0$ with $g(\cdot) > 0$ and $I(\cdot) > 0$, so an integral of a positive function up to $T_0$ is greater than or equal to the integral up to $T(1,0,t_0)$.

$$\begin{aligned} T_0 - T(1,0,t_0) &< \sqrt{-\frac{\partial T(b)}{\partial b}\Big|_{b=0}} \sqrt{\int_{t_0}^{t_0+T_0} I(t)dt} \\ &< \sup_{t^* \in \mathbb{R}} \sqrt{-\frac{\partial T(b)}{\partial b}\Big|_{b=0}} \sqrt{\int_{t^*}^{t^*+T_0} I(t)dt} \end{aligned}$$

This is the upper bound we were looking for: it limits how much the input $I(t)$ can shorten the interval between spikes in terms of the sensitivity of that interval to variation in tonic drive and the charge carried by $I(t)$ for $t \in (0, T_0)$.

The phase response curve $\Delta(\Theta)$ represents the period-shortening effect of a pulse arriving when the oscillator is at phase $\Theta$. The analysis above did not restrict us to pulsatile input; however, if $I(t)$ consists of a pulse carrying charge $K$ beginning at time 0, then for the pulse to arrive at phase $\Theta$, the system must be initialized time $t_\Theta$ before the pulse arrives. In other words, $t_0 = -t_\Theta$, and

$$\Delta(\Theta) = T_0 - T(1,0,-t_\Theta) < \sup_{t^* \in \mathbb{R}} \sqrt{-\frac{\partial T(b)}{\partial b}\Big|_{b=0}} \sqrt{\int_{t^*}^{t^*+T_0} I(t)dt} \leq \sqrt{-\frac{\partial T(b)}{\partial b}\Big|_{b=0}} \sqrt{K}$$

9.3. **Appendix: QIF neuron is not well-suited to CTC.** [[[Rewrite given familiarity with finite resets]]]

Here we show that a QIF neuron inhibiting a local network and driven by large periodic pulses does not align properly with the forcing pulses for CTC to occur. The forced QIF neuron is described by the ODE

$$\tau \dot{V} = V^2 + B + I(t)$$

where $B > 0$ is a baseline tonic drive that makes the neuron an oscillator and $V$ resets to $V_R$ after spikes, i.e. after it blows up. When unforced and initialized at $V_R$, this system is solved by

$$V_t = \sqrt{B} \tan(\frac{B}{\tau} t + \tan^{-1}(\frac{V_R}{\sqrt{B}})) \tag{37}$$

and its phase can be written

$$\mathbf{\Theta}(V) = \int_{V_R}^{V} \frac{\tau}{v^2 + B} dv = \frac{\tau}{B}(\tan^{-1}(\frac{V}{\sqrt{B}}) - \tan^{-1}(\frac{V_R}{\sqrt{B}})).$$

If $I(t)$ is a sharp pulse of duration $\delta$ carrying charge $K$ that arrives when $V = V_0$ and $\Theta = \Theta_0$, then $V$ resets to $V_0 + \frac{K}{\tau}$. The pulse resets the phase to

$$\mathbf{\Theta}(V_0 + \frac{K}{\tau}) = \frac{\tau}{B}(\tan^{-1}(\frac{V_0 + \frac{K}{\tau}}{\sqrt{B}}) - \tan^{-1}(\frac{V_R}{\sqrt{B}}))$$

$V$ was unforced until the pulse, so it took time $t = \Theta_0$ to reach $V_0$. Substituting this into (37),

$$\begin{aligned}
=&\frac{\tau}{B}(\tan^{-1}(\frac{\sqrt{B}\tan(\frac{B}{\tau}\Theta_0 + \tan^{-1}(\frac{V_R}{\sqrt{B}})) + \frac{K}{\tau}}{\sqrt{B}}) - \tan^{-1}(\frac{V_R}{\sqrt{B}}))\\
=&\frac{\tau}{B}(\tan^{-1}(\tan(\frac{B}{\tau}\Theta_0 + \tan^{-1}(\frac{V_R}{\sqrt{B}})) + \frac{K}{\tau\sqrt{B}}) - \tan^{-1}(\frac{V_R}{\sqrt{B}}))
\end{aligned} \tag{38}$$

This phase transition curve is graphed in Figure **??** with $V_R = 0$, $K = 0.1$, $B = 0.1$, and $\tau = 1$. Its intersection with the green line $\mathbf{\Theta}(V_0 + \frac{K}{\tau}) = \Theta_0 + 2$ represents a phase lock with a periodic pulse with period $T_I = T_0 - 2$. The slope at this intersection is in $(0, 1)$ so the phase lock is stable. At this intersection, pulses arrive at $\Theta_0 \approx 5$ms and reset the phase to $\Theta \approx 7$ms, still more than half a period away from a spike. Though this is perhaps an extreme case, it is representative of the fact that even spiking models subjected to periodic excitatory forcing may not phase lock with pulses arriving just before spikes. If the spikes of this neuron were inhibiting a local network, pulses would arrive while inhibition was still high, preventing CTC.

9.4. **Appendix: PRCs depend continuously on timescale separations.** Here we prove Theorem 7.0.1 from Section 7:

**Theorem 7.0.1.** *Let* (4) *be forced by a short pulse such that the PTC $F(\Theta)$ takes the form described in Theorem 4.2.1 with $\hat{\Theta} < T(0)$. Let $F_\mu(\Theta)$ denote its PTC for a given time scale separation $\mu > 0$. Let $D_\mu(\Theta)$ denote the diagonal line*

$$D_\mu(\Theta) = \Theta + q_\mu$$

*where $q_\mu$ is some continuous function of $\mu$. If $q_0 \in (0, T(0) - \hat{\Theta})$, there exists $\mu^* \geq 0$ such that for $\mu \in [0, \mu^*]$, $D_\mu(\Theta)$ intersects $F_\mu(\Theta)$ only twice: once in a $\mu$-small neighborhood of $\hat{\Theta}$ where $F'_\mu(\Theta) > 1$, and once at some $\Theta > \hat{\Theta}$ such that $|F_\mu(\Theta) - T(\mu)|$ and $|F'_\mu(\Theta)|$ are both $\mu$-small.*

*If $q_0 > T(0) - \hat{\Theta}$ or $q_0 < 0$, there exists $\mu^* \geq 0$ such that for $\mu \in [0, \mu^*]$, no intersection between $D_\mu(\Theta)$ and $F_\mu(\Theta)$ occurs.*

*Proof.* Illustrations associated with this proof are given in Figure 11.

In the following, $O(\cdot)$ is used to describe functions bounded above by a constant multiple of the argument, whereas $o(\cdot)$ is used to describe functions bounded similarly below.

For time scale separation $\mu \geq 0$, let $\Theta_0$ denote an initial phase on the stable limit cycle $(V^\mu_{\Theta_0}, s_{\Theta_0})$; we have $s_{\Theta_0} = e^{-\Theta_0}$, or $\Theta_0 = \ln\left(\frac{1}{s_{\Theta_0}}\right)$. Let $(\tilde{V}^\mu_{\Theta_0}, s_{\Theta_0})$ denote the state reached at the end of a pulse of width $\delta \ll 1$ arriving at phase $\Theta_0 - \delta$. During a pulse, $s$ only changes by $O(\mu)$, so the large, positive vector field for $V$ only changes by $O(\mu)$; therefore the final state $\tilde{V}^\mu_{\Theta_0}$ is $O(\mu)$-close to $\tilde{V}^0_{\Theta_0}$.

Given a diagonal line $D_\mu(\Theta) = \Theta + q_\mu$ with $q_0 \in (0, T(0) - \hat{\Theta})$, we restrict the stable and unstable branches $V^-(b - gs)$ and $V^+(b - gs)$ by bounding them at $s = \frac{b}{g}e^{\frac{q_0}{2}}$, henceforth referred to as the "branch boundary." (See Figure 11, right.) Within these bounds, the branches are normally attracting/repelling for $\mu = 0$, so by Fenichel's persistence theorem [**Fenichel**], they perturb into

slow attracting and repelling manifolds $V_\mu^-(b-gs)$ and $V_\mu^+(b-gs)$, both $\mu$-close to the original branches.

For an intersection of $D_\mu$ and $F_\mu$ to occur, we must have

$$\begin{aligned} D_\mu(\Theta_0) =& F_\mu(\Theta_0) \\ \Theta_0 + q_\mu =& \mathbf{\Theta}\left(\tilde{V}^\mu_{\Theta_0}, s_{\Theta_0}\right) = T(\mu) - T_s\left(\tilde{V}^\mu_{\Theta_0}, s_{\Theta_0}\right) \\ T_s\left(\tilde{V}^\mu_{\Theta_0}, s_{\Theta_0}\right) =& T(\mu) - q_\mu - \Theta_0 \end{aligned} \tag{39}$$

First, let us consider an initial phase $\Theta_0$ sufficiently far below $\hat{\Theta}$ that the pulse resets $V^\mu_{\Theta_0}$ to $\tilde{V}^\mu_{\Theta_0}$ left of the repelling manifold $V_\mu^+$. The system state must stay left of the repelling manifold until the manifold's boundary at $s = \frac{b}{g}e^{\frac{q_0}{2}}$; at this point, $s$ has decayed from $s_{\Theta_0} = e^{-\Theta_0}$ to $\frac{b}{g}e^{\frac{q_0}{2}}$, which required time $-\ln\left(\frac{b}{ge^{-\Theta_0}}e^{\frac{q_0}{2}}\right) = T(0) - \frac{q_0}{2} - \Theta_0$. Even if a spike occurs immediately, we still have

$$T_s(\tilde{V}^\mu_{\hat{\Theta}}, s_{\Theta_0}) \geq T(0) - \frac{q_0}{2} - \Theta_0.$$

By the results of Krupa and Szmolyan [16], $T(\mu)$ is $O(\mu^{\frac{2}{3}})$-close to $T(0)$:

$$T_s(\tilde{V}^\mu_{\hat{\Theta}}, s_{\Theta_0}) \geq T(\mu) - O(\mu^{\frac{2}{3}}) - \frac{q_0}{2} - \Theta_0.$$

For sufficiently small $\mu$, $q_\mu > \frac{q_0}{2} + O(\mu^{\frac{2}{3}})$, so

$$T_s(\tilde{V}^\mu_{\hat{\Theta}}, s_{\Theta_0}) \geq T(\mu) - q_\mu - \Theta_0$$

in contradiction to (39); so for this initial phase $\Theta_0$ this far below $\hat{\Theta}$, no intersection between $F_\mu(\Theta_0)$ and $D_\mu(\Theta_0)$ can occur. The same argument applies to a trajectory reset to $\tilde{V}^\mu_{\Theta_0}$ on the repelling manifold, or any trajectory initialized close enough to the right of the repelling manifold it that it passes through the branch boundary before spiking.

Next, let us consider $\Theta_0$ is large enough that $\tilde{V}^\mu_{\Theta_0}$ is right of the repelling manifold and large enough that it spikes before reaching the branch boundary. We change variables from $V$ to the Fenichel normal form $U := V - V_\mu^+(b-gs)$, representing the distance of $V$ from the repelling manifold. We use this new coordinate to split the region right of the repelling manifold and above the branch boundary into two regions: Region 1, a neighborhood of the unstable branch of width $\sqrt{\mu}$ defined by $U < \sqrt{\mu}$, and Region 2, the region defined by $U \geq \sqrt{\mu}$. We have

$$U' = \frac{1}{\mu}\left((2\sqrt{gs-b} + O(\mu))U + O(U^2)\right). \tag{40}$$

In Region 2, we have $U' = o(\frac{1}{\sqrt{\mu}})$, so trajectories pass through Region 2 in time $O(\sqrt{\mu})$, and $T_s(V,s)$ in the second region is $O(\sqrt{\mu})$. Therefore, condition (39) may be met in only two cases:

(1) $(\tilde{V}^\mu_{\Theta_0}, s_{\Theta_0})$ is in Region 1, and the trajectory remains in the first region for time $O(\sqrt{\mu})$-close to $T(\mu) - q_\mu - \Theta_0$.

(2) $(\tilde{V}^\mu_{\Theta_0}, s_{\Theta_0})$ is in Region 2, $\Theta_0$ is $O(\sqrt{\mu})$-close to $T(\mu) - q_\mu$, and $T_s(\tilde{V}^\mu_{\Theta_0}, s_{\Theta_0})$ is $O(\sqrt{\mu})$-close to zero.

We study the second case first. We immediately have

$$F_\mu(\Theta_0) = T(\mu) - T_s(\tilde{V}^\mu_{\Theta_0}, s_{\Theta_0}) = T(\mu) - O(\sqrt{\mu}),$$

so pulses arriving at such a phase $\Theta_0$ reset the system to immediately before a spike. We want to show that in this case, $F'_\mu(\Theta_0)$ goes to zero with $\mu$; as a consequence, only one intersection may occur with $D_\mu(\Theta_0)$ and this intersection corresponds to a stable phase lock with pulses arriving immediately before spikes.

We have assumed that $q_0 < T(0) - \hat{\Theta}$, and both $q_\mu$ and $T(\mu)$ depend continuously on $\mu$, so for sufficiently small $\mu$, $T(\mu) - q_\mu$ is $o(1)$ larger than $\hat{\Theta}$. In this case we have $\Theta_0$ close to $T(\mu) - q_\mu$ by assumption, so $\Theta_0$ is also $o(1)$ larger than $\hat{\Theta}$. We have

$$\tilde{U}^0_{\hat{\Theta}} := \tilde{V}^0_{\hat{\Theta}} - V^+_\mu(b - gs_{\hat{\Theta}}) = \tilde{V}^0_{\hat{\Theta}} - V^+(b - gs_{\hat{\Theta}}) + O(\mu) = O(\mu).$$

We showed in the proof of Theorem 4.2.1 that $\frac{\partial}{\partial\Theta_0}(\tilde{V}_{\Theta_0} - V^+(b - s_{\Theta_0})) > 0$ (with no dependency on $\mu$, so it is $o(1)$ greater than zero). $V^+_\mu$ is an $O(\mu)$-sized $C^1$ perturbation of $V^+$, so for sufficiently small $\mu$ we also have

$$\frac{\partial}{\partial\Theta}\tilde{U}_\Theta = \frac{\partial}{\partial\Theta}(\tilde{V}_\Theta - V^+_\mu(b - s_\Theta)) = \frac{\partial}{\partial\Theta}(\tilde{V}_\Theta - V^+(b - s_\Theta)) + O(\mu) = o(1).$$

Since $\Theta_0$ is also $o(1)$ larger than $\hat{\Theta}$, we conclude that $\tilde{U}^0_{\Theta_0}$ is $o(1)$. We showed above that $\tilde{V}^\mu_\Theta$ (and hence $\tilde{U}^\mu_\Theta$) depends continuously on $\mu$; therefore, for sufficiently small $\mu$, $\tilde{U}^\mu_{\Theta_0}$ is $o(1)$, and $U'$ at this point is $O(\frac{1}{\mu})$.

In order to show that $F'_\mu(\Theta_0)$ goes to zero with $\mu$, it is sufficient to show that $\frac{\partial}{\partial\Theta}\big|_{\Theta=\Theta_0}\mathbf{\Theta}(\tilde{V}^\mu_\Theta, s_\Theta) \to 0$ with $\mu$; equivalently, we may show that $\frac{\partial}{\partial\Theta}\big|_{\Theta=\Theta_0}T_s(\tilde{V}^\mu_\Theta, s_\Theta) \to 0$. $s$, evolving autonomously at rate $o(1)$ and $O(1)$, is a surrogate for time, so equivalently we may show that $\frac{\partial}{\partial\Theta}\big|_{\Theta=\Theta_0}(s_{\Theta+T_s} - s_\Theta \to 0$, where $s_{\Theta+T_s}$ is the value of $s$ when a trajectory initialized at $(\tilde{V}^\mu_\Theta, s_\Theta)$ reaches $V_{spike}$.

This last condition is easily demonstrated by normalizing the vector field such that all vectors have length one. All trajectories of the normalized vector field trace out the same paths in $(V, s)$-space as those of the unnormalized vector field. In Region 2, $U'$ (and hence $V'$) is arbitrarily large for sufficiently small $\mu \geq 0$; so the normalized vector field approaches rightward horizontal normalized vector field [[[IN C1?]]], and the curve $(\tilde{V}^\mu_{\Theta_0}, s_{\Theta_0})$ is transverse to the normalized vector field, as is the (flat) curve $V = V_{spike}$. Thus, $s_{\Theta_0+T_s}$ approaches $s_{\Theta_0}$ in $C^1$, and $\frac{\partial}{\partial\Theta}\big|_{\Theta=\Theta_0}(s_{\Theta+T_s} - s_\Theta) \to 0$. Therefore $F'_\mu(\Theta_0)$ goes to zero with $\mu$.

Next, we study the first case: $(\tilde{V}^\mu_{\Theta_0}, s_{\Theta_0})$ is in Region 1, and the trajectory remains in the first region for time $O(\sqrt{\mu})$-close to $T(\mu) - q_\mu - \Theta_0$. We want to show that in this case, $F'_\mu(\Theta_0)$ goes to infinity as $\mu \to 0$; as a consequence, $F_\mu(\Theta)$ can only intersect $D_\mu(\Theta)$ at one such $\Theta_0$ and this intersection cannot correspond to a stable phase lock.

First, we note that for the system to spend $o(1)$ time in $\sqrt{\mu}$-wide Region 1 (as it must, in this case, by assumption), the vector field must point almost directly along the repelling manifold, and in particular must be transverse to the curve $(\tilde{U}^\mu_\Theta, s_\Theta)$; otherwise trajectories initialized along that curve would exit Region 1 in time $O(\sqrt{\mu})$. Therefore, for small $\epsilon$, trajectories initialized at $(\tilde{U}^\mu_{\Theta_0}, s_{\Theta_0})$ and $(\tilde{U}^\mu_{\Theta_0+\epsilon}, s_{\Theta_0+\epsilon})$ remain $O(\epsilon)$ separate in the $U$-direction when the first is allowed to flow forward for time $O(\epsilon)$ to meet the second at $s = s_{\Theta_0+\epsilon}$.

We study dynamics in Region 1 by approximating the expansion in the variable $U$. We see by differentiating (40) by $U$ that $U$ is expanding exponentially at a rate of $\frac{2}{\mu}(\sqrt{gs-b}+O(\mu)+O(U)) = o(\frac{1}{\mu})$ while it remains in Region 1. Thus, if two $\epsilon$-close trajectories initialized at the same value of $s$ spend a specific $o(1)$ amount of time in Region 1 (as they do, in this case, by assumption), they separate in the $U$-direction by a factor of $e^{\frac{C}{\mu}}$ for some constant $C$. Trajectories exit Region 1 with slope $U' = o(\frac{1}{\sqrt{\mu}})$, so their $o(\epsilon e^{\frac{C}{\mu}})$ separation in the $U$-direction becomes a separation of $o(\epsilon\sqrt{\mu}e^{\frac{C}{\mu}})$ in the $s$-direction, still exponentially large with small $\mu$.

These trajectories enter Region 2 transversely and reach $V_{spike}$ transversely, so as demonstrated above by normalizing the vector field, their time to cross Region 2 as a function of initial state is $\mu$-close to zero in $C^1$; therefore the $o(\epsilon\sqrt{\mu}e^{\frac{C}{\mu}})$-separation of trajectories in the $s$-direction becomes an $o(\epsilon\sqrt{\mu}e^{\frac{C}{\mu}})$-separation in spike time. We conclude that a trajectory receiving a pulse at phase $\Theta_0+\epsilon$ spikes $o(\epsilon\sqrt{\mu}e^{\frac{C}{\mu}})$ later than the trajectory receiving a pulse at $\Theta_0$; equivalently, the difference between $T_s(\tilde{V}^{\mu}_{\Theta_0}, s_{\Theta_0})$ and $\mathbf{\Theta}(\tilde{V}^{\mu}_{\Theta_0}, s_{\Theta_0})$, the times for each trajectory to spike after the end of their respective pulses, is $o(\epsilon\sqrt{\mu}e^{\frac{C}{\mu}} - \epsilon)$. Thus, the slope of $F_\mu(\Theta)$ in this range is arbitrarily large as $\mu \to 0$.

□

9.5. **Appendix: Reconciling our results with experiment.** In Figure 12, we reproduce the phase response curves measured by Akam et al. in [1]. In Figure 13, we show that their model produces spike-or-forget results very similar to ours if the input is assumed to be excitatory. We also note that the PRCs in Figure 12 both have long, shallow downward slopes that cause a wide range of phases to be reset to the same phase, which in the case of alveus stimulation is the phase of minimal inhibition immediately preceding the excitatory trough just like the PRCs presented here.

## 10. References


[1] Thomas E Akam et al. "Oscillatory dynamics in the hippocampus support dentate gyrus âĂŞ CA3 coupling". In: *Nature neuroscience* 15.5 (2012), pp. 763–768.

[2] Bassam V Atallah and Massimo Scanziani. "Instantaneous Modulation of Gamma Oscillation Frequency by Balancing Excitation with Inhibition". In: *Neuron* 62.4 (2009), pp. 566–577.

[3] Christoph Börgers. "Synchronization in Networks of Excitatory and Inhibitory Neurons with Sparse, Random Connectivity". In: 538 (2003), pp. 509–538.

[4] Christoph Börgers and Nancy J Kopell. "Effects of noisy drive on rhythms in networks of excitatory and inhibitory neurons." In: *Neural computation* 17.3 (Mar. 2005), pp. 557–608.

[5] Christoph Börgers and Nancy J Kopell. "Gamma oscillations and stimulus selection." In: *Neural computation* 20.2 (Feb. 2008), pp. 383–414.

[6] Christoph Börgers et al. "Minimal Size of Cell Assemblies Coordinated by Gamma Oscillations". In: *PLoS Computational Biology* 8.2 (2012).

[7] György Buzsáki and Xiao-Jing Wang. "Mechanisms of gamma oscillations." In: *Annual review of neuroscience* 35 (Jan. 2012), pp. 203–25.

[8] Carson C Chow et al. "Frequency control in synchronized networks of inhibitory neurons." In: *Journal of computational neuroscience* 5.4 (Dec. 1998), pp. 407–20.

[9] Jozsef Csicsvari et al. "Mechanisms of gamma oscillations in the hippocampus of the behaving rat." In: *Neuron* 37.2 (Jan. 2003), pp. 311–22.

[10] Neil Fenichel. "Persistence and Smoothness of Invariant Manifolds for Flows". In: *Indiana University Mathematics Journal* 21.3 (1971), pp. 193–226.

[11] Stan Gielen, Martin Krupa, and Magteld Zeitler. "Gamma oscillations as a mechanism for selective information transmission". In: *Biological Cybernetics* (2010), pp. 151–165.

[12] Nathan W Gouwens et al. "Synchronization of firing in cortical fast-spiking interneurons at gamma frequencies: a phase-resetting analysis." In: *PLoS computational biology* 6.9 (Jan. 2010).

[13] Eugene M Izhikevich. "Simple model of spiking neurons." In: *IEEE transactions on neural networks* 14.6 (Jan. 2003), pp. 1569–72.

[14] Jan Karbowski and Nancy J Kopell. "Multispikes and synchronization in a large neural network with temporal delays." In: *Neural computation* 12.7 (July 2000), pp. 1573–606.

[15] Zachary P Kilpatrick and G Bard Ermentrout. "Sparse Gamma Rhythms Arising through Clustering in Adapting Neuronal Networks". In: *PLoS Computational Biology* 7.11 (Nov. 2011). Ed. by Boris S. Gutkin, e1002281.

[16] M Krupa and P Szmolyan. "Extending geomentric singular perturbation theory to nonhyperbolic points – fold and canard points in two dimensions". In: *SIAM Journal on Applied Mathematical Analysis* 33.2 (2001), pp. 286–314.

[17] Pierre Sacré. "Systems analysis of oscillator models in the space of phase response curves". PhD thesis. 2013.

[18] Eli Shlizerman and Philip Holmes. "Neural dynamics, bifurcations, and firing rates in a quadratic integrate-and-fire model with a recovery variable. I: Deterministic behavior." In: *Neural computation* 24.8 (Aug. 2012), pp. 2078–118.

[19] Dorea Vierling-Claassen and Nancy J Kopell. "The Dynamics of a Periodically Forced Cortical Microcircuit, With An Application to Schizophrenia". In: 8.2 (2009), pp. 710–733.

[20] Carl van Vreeswijk. "Partial synchronization in populations of pulse-coupled oscillators." In: *Physical review. E, Statistical physics, plasmas, fluids, and related interdisciplinary topics* 54.5 (Nov. 1996), pp. 5522–5537.

[21] Xiao-jing Wang and György Buzsáki. "Gamma oscillation by synaptic inhibition in a hippocampal interneuronal network model." In: *Journal of Neuroscience* 16.20 (Oct. 1996), pp. 6402–13.

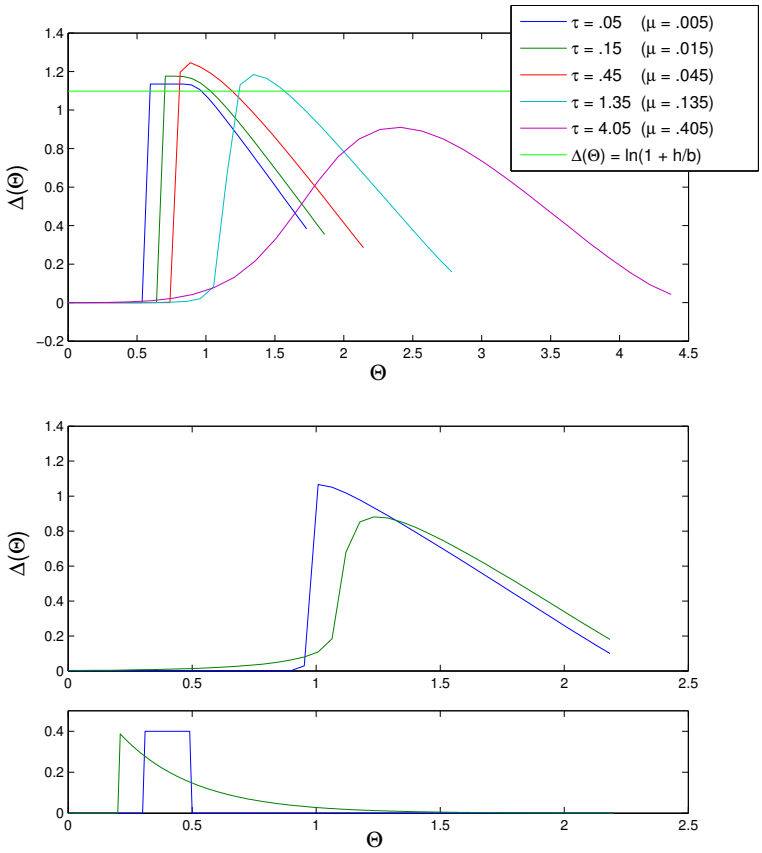


Figure 10: **Beyond the singular limit.** Phase response curves produced by simulation of the ODE (1) with $g = 1, \tau_s = 10$. **Top:** $\mu = \frac{\tau}{\tau_s}$ is changed by letting $\tau$ range from .05 to 4.05, while the forcing pulse remains the same ($\delta = 4$, $h = .5$. As $\mu$ increases, $\Delta(\Theta)$ varies continuously with $\mu$, while the qualitative properties of the PRC remain similar. The most dramatic change is the rapid growth of the natural period, and the resulting increase in the domain of $\Delta(\Theta)$. At first, the increasing period allows the PRC to grow slightly above its theoretical maximum for $\mu = 0$ (bright green). Then the larger value of $\tau$ makes the pulse less effective, and the height of the PRC decreases. On the right side of their domains, PRCs do not return fully to zero due to non-instantaneous pulses: when a spike occurs before the end of a pulse, the asymptotic phase at the end of the pulse is beyond $T(\mu)$, so the PRC can be positive even at $\Theta_0 = T(\mu)$. Visual inspection shows that for most horizontal lines in the range of the PRCs, two intersections occur: one with positive slope (an unstable phase locking phase) and one with slope approximately $-1$ (a stable phase locking phase). **Bottom:** The phase response curve for an excitatory pulse with sudden onset and exponential decay with time constant $3ms$ is qualitatively very similar to the PTC for a square pulse.

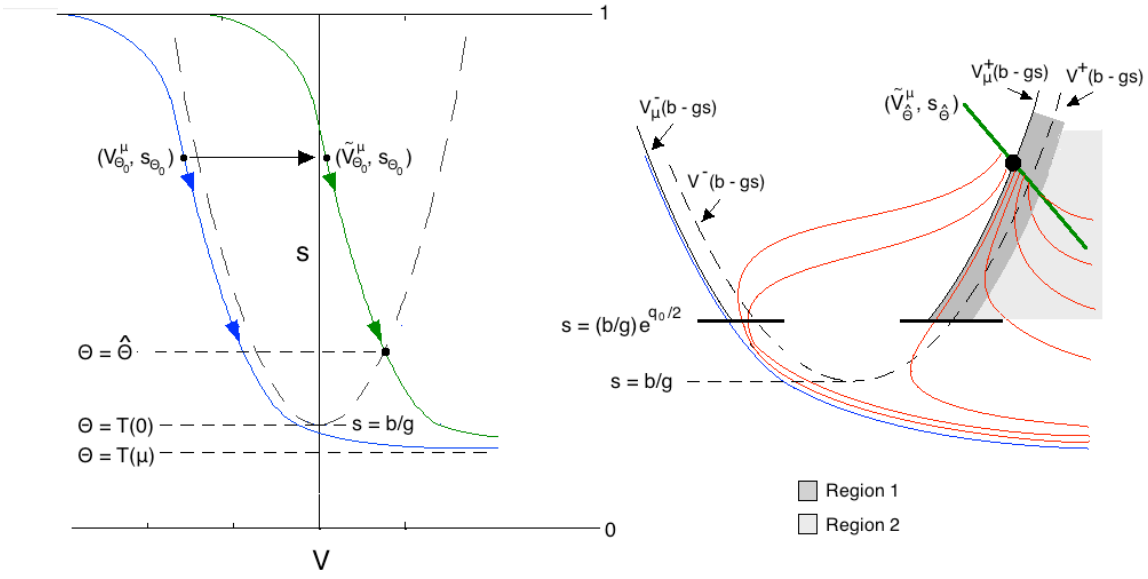


Figure 11: Illustration of the definitions in the proof of Theorem 7.0.1.

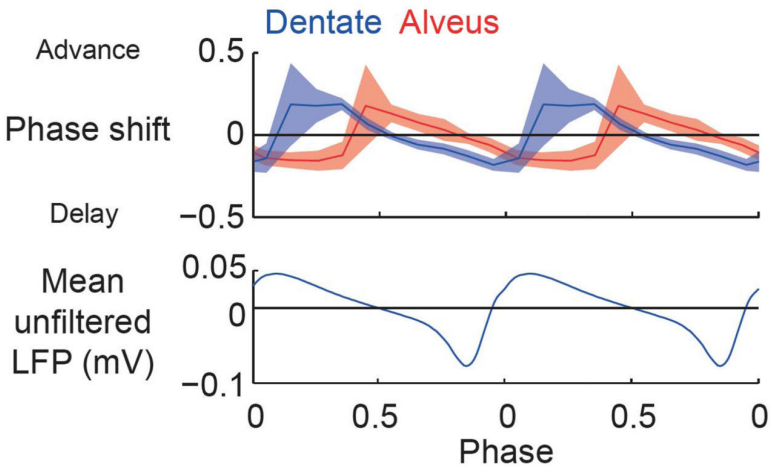


Figure 12: Phase response curves measured in the CA3 region by Akam et al. in [1] in response to electrical stimulation to the alveus and dentate gyrus. They show that stimulation may also delay gamma phase, presumably due to directly activating a subset of the inhibitory interneurons in a PING circuit; here we focus on the effects of directly activating either the complete inhibitory population or enough E-cells to evoke a full inhibitory volley.

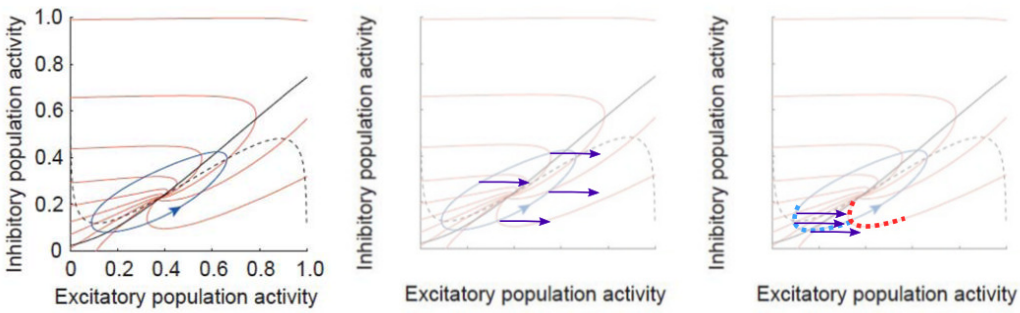


Figure 13: **Left:** In [1], a Wilson-Cowan model is proposed to explain the PRCs observed when stimulating the hippocampus during gamma rhythms. Overall levels of excitation and inhibition fluctuate in a gamma-rhythm cycle; the effects of electrical perturbations are reproduced when stimulations are assumed to be primarily inhibitory. If excitation is instead assumed to be entirely excitatory, their model agrees qualitatively with the PRCs analytically described here. **Middle:** A strong excitatory perturbation at these phases does not carry the system more than one isochron forward or back; these phases correspond to the first case in expression (**??**), where stimulation is not strong enough to evoke a spike, and instead has no effect on the oscillator's phase. **Right:** A strong excitatory perturbation at these phases on the limit cycle (dotted blue curve) carries the system onto a single isocline (dotted red curve) representing an asymptotic phase just before peak excitatory activity; these phases correspond to the second case in (**??**), where stimulation is strong enough to evoke a spike immediately.